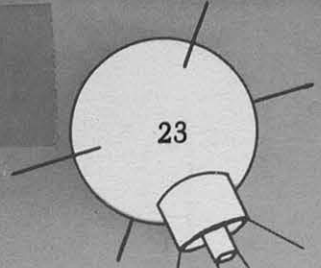

MESOMETEOROLOGY PROJECT

Department of the Geophysical Sciences
The University of Chicago

THE MESOANALYSIS OF AN ORGANIZED CONVECTIVE SYSTEM

by

Henry Albert Brown

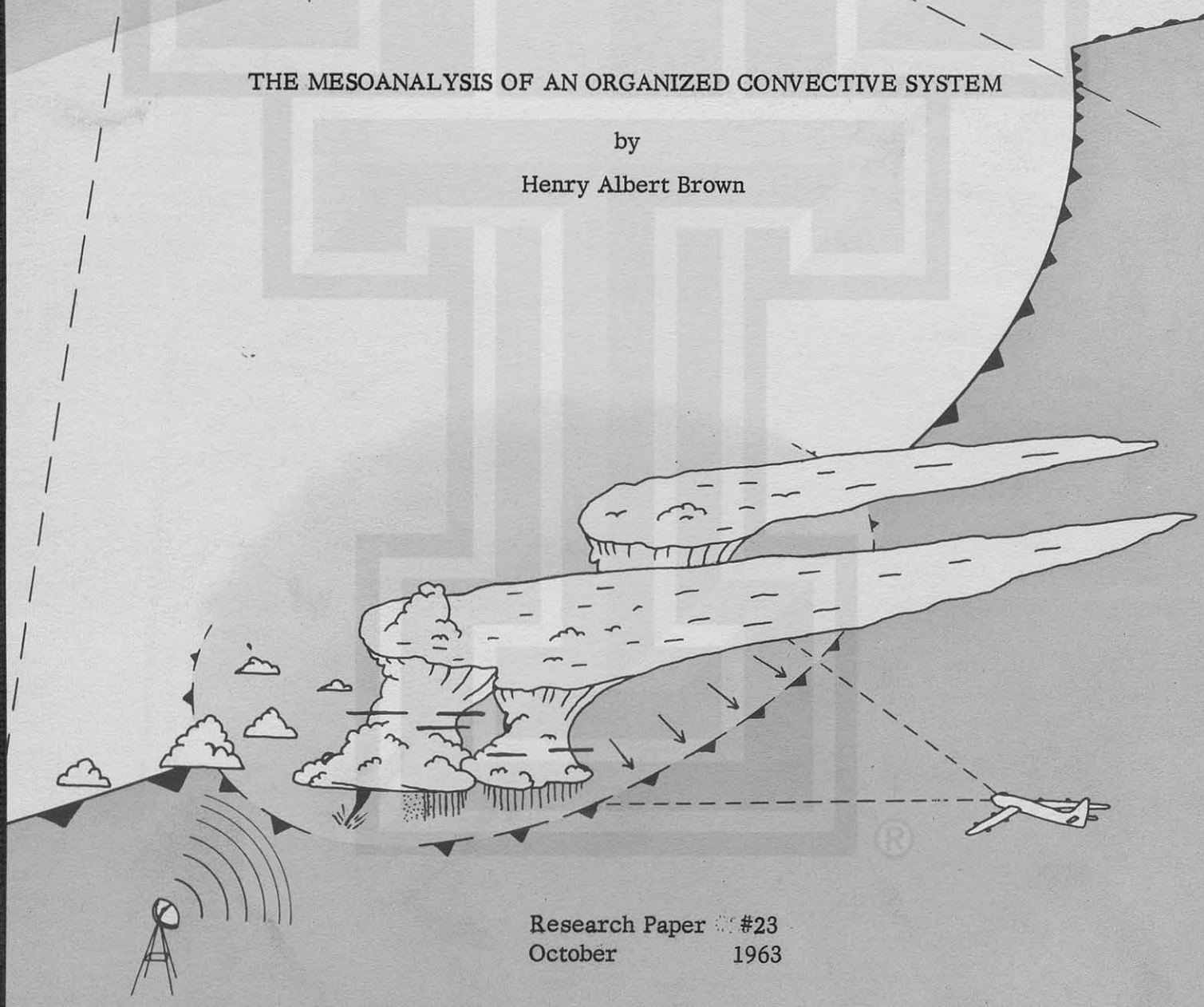

Research Paper #23
October 1963

MESOMETEOROLOGY PROJECT ------- RESEARCH PAPERS

1. Report on the Chicago Tornado of March 4, 1961 - Rodger A. Brown and Tetsuya Fujita *

2. Index to the NSSP Surface Network - Tetsuya Fujita *

3. Outline of a technique for Precise Rectification of Satellite Cloud Photographs - Tetsuya Fujita *

4. Horizontal Structure of Mountain Winds - Henry A. Brown *

5. An Investigation of Developmental Processes of the Wake Depression Through Excess Pressure Analysis of Nocturnal Showers - Joseph L. Goldman *

6. Precipitation in the 1960 Flagstaff Mesometeorological Network - Kenneth A. Styber *

7. On a Method of Single- and Dual-Image Photogrammetry of Panoramic Aerial Photographs - Tetsuya Fujita (To be pub lished)

8. A Review of Researches on Analytical Mesometeorology - Tetsuya Fujita

9. Meteorological Interpretations of Convective Nephsystems Appearing in TIROS Cloud Photographs - Tetsuya Fujita, Toshimitsu Ushijima, William A. Hass, George T. Dellert, Jr.

10. Study of the Development of Prefrontal Squall-Systems Using NSSP Network Data - Joseph L. Goldman

11. Analysis of Selected Aircraft Data from NSSP Operation, 1962 - Tetsuya Fujita

12. Study of a Long Condensation Trail Photographed by TIROS I - Toshimitsu Ushijima

13. A Technique for Precise Analysis of Satellite Data; Volume I - Photogrammetry - (Published as MSL Report No. 14) - Tersuya Fujita

14. Investigation of a Summer Jet Stream Using TIROS and Aerological Data - Kozo Ninomiya

15. Outline of a Theory and Examples for Precise Analysis of Satellite Radiation Date - Tetsuya Fujita

* Out of print

(Continued on back cover)

MESOMETEOROLOGY PROJECT

Department of the Geophysical Sciences

The University of Chicago

THE MESOANALYSIS OF AN ORGANIZED CONVECTIVE SYSTEM*

by

Henry Albert Brown

RESEARCH PAPER #23

* Reprinted from Mesometeorological Study of Selected Areas in the United States, Final Report to the U. S. Army Signal Corps under Contract No. DA 36-039 SL-88932.

Table of Contents

The Mesoanalysis of an Organized Convective System

Henry Albert Brown

Abstract

The mesoanalysis of an organized convective system which originated in New Mexico on May 29, 1960, and propagated into eastern Texas on May 30, is presented. Special attention is given to observed cloud patterns and some methods of cloud analysis described. Rectification of TIROS I photographs which were taken on May 30 revealed the cloud structure of the dissipating squall line.

The time variations of pressure and humidity with respect to the squall line are examined, and comparisons are made of the variations. In addition, the vertical motion field during the period of maximum development of the squall line is computed and described.

1. INTRODUCTION

Organized convective systems ranging in size from tens to hundreds of miles represent one of the most difficult and least understood of meteorological problems. Their importance in terms of local weather effects and therefore, short- and medium-range forecasting would be difficult to overestimate.

Radar, utilized as a weather instrument, first outlined the origins of these systems and their tendency for organization. It has since served as a major source of information concerning their characteristics. Another instrument which has served in a most useful capacity is the microbarograph. Following the establishment of the Severe Storms Network in the Midwestern United States, this instrument has furnished the major portion of surface data suitable for the detailed examination of mesosystems.

Analyses utilizing this type of data have revealed many of the characteristics of

the squall line mesosystems. The variation of the excess pressure produced by the system during its lifetime has led to the recognition (Fujita, 1955, Fujita and Brown, 1957), of three stages of development in the squall line. These stages when correlated with precipitation produced by the system have led to a more complete understanding of the processes involved.

It is unfortunate that the most detailed observations available are limited to the surface of the earth. Thus, it is only that the surface manifestations of upper level disturbances have been given detailed analytical study. In terms of direct evidence concerning the upper level details of the mesoscale systems very little information, except for radar, is to be had. The mesoanalyst is therefore faced with the problem of making full and complete use of all surface information that is available, obtaining as much information as possible on the upper level disturbances and processes through indirect evidence of the varied surface measurements, and utilizing all upper level data that can be obtained for a more complete physical understanding of mesoscale weather processes.

The present paper is an attempt to fulfill these conditions in the detailed analysis of a mesosystem. The first objective of the study is the analysis of the squall line systems using the conventional parameters, e. g. pressure, wind, temperature and precipitation. In addition to these an additional surface parameter, the relative humidity, will be utilized. The existence of phenomena known as the humidity dip was first shown in The Thunderstorm (1947). Its possible causes were discussed and its relation to various parameters noted. More recently, Brown (1962), presented evidence that the humidity dip could also be a mesoscale phenomenon and discussed the implications of the presence of such a phenomenon within the squall line system. The variation of the humidity dip with respect to the life cycle of the squall line remained an unknown quantity,and one of the purposes of this paper is to examine this variation.

The upper air data utilized in the report consists of the conventional upper air network and its six- and twelve-hourly observations. Fortunately, the mesosystem was located in a more or less ideal position with respect to the network at one observation time (0600 CST, May 30, 1960) and consequently large scale upper-level convergence and divergence patterns and the resulting vertical motion patterns with

respect to the squall line and its environment could be obtained. With regard to the last condition imposed, namely the use of all upper level data, it was discovered that the TIROS I satellite was orbiting the area during the period under study. The rectification of the photographs using a technique developed by Fujita (1961) revealed in remarkable detail the cloud pattern of the dissipating stages of a mesosystem.

2. CASE STUDY OF MAY 29-30, 1960

The choice of the Texas-New Mexico area during the period of 1800 CST, May 29 until 1800 CST, May 30, 1960 as an area of study was determined by preliminary precipitation analysis and by reference to the orbit data of TIROS I (1961). An additional criterion that was imposed was the absence of a front in the area of mesoscale activity. The large scale weather features that existed prior to the initiation of activity consisted of a large surface anticyclone situated over the Oklahoma-Kansas area and a low pressure area over Arizona and western New Mexico. The surface wind field was strongly divergent throughout Oklahoma, Texas and eastern New Mexico. However, forced lifting of surface air was apparent throughout western Texas and eastern New Mexico due to the strong easterly component of the surface winds and the topographic upslope to the west.

A. MESOANALYSES

The total precipitation produced by the storm of May 29-30, Fig. 1, illustrates the concentration of precipitation along a narrow zone. The hourly positions of maximum precipitation centers indicate the origin of the system at about 1800 CST in the vicinity of Mt. Taylor (11389'), just to the west of Albuquerque, New Mexico. The system then proceeded to organize, expand and move to the east southeast at about 30 mph. Maximum development, as shown by the areal extent of heavy precipitation, occurred at about 08-0900 CST. A secondary development occurred in the southwest sector of the Panhandle at about 0900 CST. A small precipitation maximum, starting at 1000 CST and extending in time to 1600 CST, was found to be a new development which occurred to the south of the maximum precipitation center. The southern branch of the split dissipated shortly after 1000 CST while the eastern branch

continued to produce considerable activity until approximately 1600 CST.

Hourly mesoanalyses produced detailed features of the squall line mesosystem as it moved eastward through Texas. Examples, Fig. 24, at six hourly intervals show the mesosystem at three stages of its development. The formative stage at 0300 CST, Fig. 2a and 2b, is illustrated by the sharp pressure jump line, narrow band of intense precipitation and the appearance of a mesolow pressure to the rear of mesohigh. The shaded zone along and just to the rear of the leading edge of the system marks a zone where humidities were less than 100 percent even though precipitation was occurring. This mesoscale zone, described by Brown (1962), is characterized as a "humidity dip".

The mature stage of the system is shown at 0900 CST, Fig. 3a and 3b. The areal expansion of the system, the increased development of the low and high, and the widespread but still intense precipitation band denotes mature mesosystem. The existence and continued expansion of the humidity dip at this time was still apparent.

The dissipating stage of the system, Fig. 4c and 4b, is characterized almost 24 hours after its initial development by diminishing areas of precipitation, weakening of high and low pressure areas, and the disappearance of the humidity dip.

3. MESOSCALE CLOUD SYSTEMS

The patterns of clouds which are produced by large-scale weather systems have been a subject of much interest to meteorologists. Models which were adapted to large-scale frontal systems have undergone some revision with the advent of the TIROS satellites.

Cloud patterns of mesoscale systems, e.g., cloud streets, hurricane rainbands, squall lines, etc., have been known to exist for many years, but little analysis was possible because of the lack of proper observational instruments. The TIROS satellites proved to be exceptionally good observers of mesoscale cloud structure. One of the first identifications of the origin of a mesosystem was made by Whitney and Fritz (1961) following the rectification and study of a "square" cloud. The realization that the distribution or patterns of clouds of a squall-line mesosystem must

undergo an evolutionary process which is connected with the life cycle process of the mesosystem is not new. However, not until the TIROS photographs were available has it been possible to examine the cloud systems in such detail.

In order to coordinate the surface analyses with TIROS photographs, cloud charts were plotted and analysed for each hour of the study. Examples of the developing and mature stage are shown in Fig. 5a and 5b. The cloud cover and height symbols are explained in the legend of Fig. 5a. The legend of Fig. 5b represents the manner in which an assumption was applied in order to obtain more detail in the cloud analysis. This assumption, a common one in mesometeorological techniques, also allows for an increase in the amount of data available for a given analysis.

The assumption is that the individual change of an element, in this case the cloud systems, is approximately zero and that the local change observed in cloudiness is due entirely to advection. Thus, the cloud observations can be adjusted over a short period of time as shown in the legend of Fig. 5b. The scattered symbols (high, middle and low-level clouds) are assumed representative of observations at a time, t - 1 hour. The broken symbols (high, middle and low) in the center circle, or location of observation site, are assumed observations at the time t. The observations at time t + 1 hour are indicated by the broken and overcast symbols to the left and bottom of the center observation figure. A space representation of the cloud cover is thus given which would indicate low clouds moving from the south and increasing in amount to the south, middle clouds moving from the west and the amount symbols indicating an increasing middle cloud cover to the west, and finally, high clouds moving from the southwest and increasing to overcast conditions in the southwest. The speed of movement would govern the distance from the station observation site at the time t and the direction of movement would govern the orientation of the line along which the clouds are plotted. In the legend, the clouds are all shown with a movement of approximately 25 mph. After various trials in the cloud analysis it was decided that due to the increased simplicity and predominantly westerly flow aloft that the observations could all be oriented from west to east. Thus, the observations for a given station are grouped in three circles, the latest observation (t + 1) to the left, the current (t) at the center and the earliest (t - 1) to the right.

The cloud cover symbols and the cloud height indicators indicate the increase in cloudiness and the decrease in cloud elevations on approaching the mesosystem from the east. In addition an examination of the charts very clearly shows the expansion of the cloud system with time. The upper, or cirrus, layer is perhaps the most striking feature of the system expansion. The low cloud area which was an elliptical-shaped area in the early stages of the system development became elongated or stretched into a somewhat U-shaped area by 0900 CST.

4. RECTIFICATION OF SATELLITE PHOTOGRAPHS

On May 30, 1960, TIROS I passed over the Midwestern United States in its 863rd orbit. The one-minute positions of the satellite, Fig. 6, beginning at 1620 CST (2220 GCT) indicate a track between Salt Lake City and Havana, Cuba. On a direct readout mode, six pictures were taken at half-minute intervals beginning at 1622 CST (2222 GCT), indicated by the black arrow.

The photographs were rectified utilizing a method developed by Fujita (1961). In order to simplify the interpretation of the cloud positions and areas of coverage, the boundaries of the states were superimposed on the photographs. Thus, the first two photographs, Fig. 7a and 7b, clearly indicate the widespread cumuliform cloudiness over the mountainous areas in the state of Wyoming, extending southward into Utah and Colorado. Of particular interest are the clouds over western Nebraska and South Dakota separated from the Wyoming cloudiness by a relatively sharp clear zone. The greatest contrast in the clouds is between the scattered unorganized smaller cumuliform clouds over Wyoming, Colorado and Utah (mountainous areas), and the larger apparently organized masses of cumuliform clouds over Nebraska and South Dakota (plains area). The cloud masses of the mountains show relatively sharp edges while the plains clouds indicate the fuzzy, fibrous structure of the cirrus shield. Weather observations from stations in the vicinity, e.g., Goodland, Kansas, indicate the presence of large cumulonimbi to the northwest, while mountain stations, e.g., Grand Junction, indicated cumulonimbi in all quadrants. The third picture, Fig. 8a, taken 30 seconds later showed the smaller cumuliform cloud masses over the mountainous areas extending south into Colorado and the larger cumuliform masses line

up north-south along the Wyoming-Nebraska-South Dakota borders. The cirriform shield from the cloud mass located in southeastern Wyoming and western Nebraska extends approximately 150 miles in an east-west direction and 50 miles in the north-south, truly a mesoscale cloud system. The similarity of this cloud system to the large cumulonimbi in photographs made by Cunningham (1960) is striking.

Thirty seconds later, the fourth picture, Fig. 8b, was taken and revealed additional cloud structure and patterns over New Mexico and western parts of Texas, Oklahoma and Kansas, and a large clear area in Kansas and central Nebraska. The large cloud mass in New Mexico is located in approximately the same position that the mesosystem, (studied in this case) originated approximately 24 hours earlier. Smaller cumuliform masses are located in west Texas and southeast New Mexico.

The fifth and sixth, and last, photographs in the series, Fig. 9a and 9b, revealed additional information concerning cloud structure in central Texas and all of Oklahoma. Of special interest is the large, predominantly cirriform, cloud mass centered in central Oklahoma and fanning out into southeast Kansas, western Missouri, Arkansas and northeast Texas.

Reference to the previous surface pressure, precipitation and cloud charts reaffirms that the organized convective system which originated in New Mexico some 22 hours earlier had passed through its mature stage and was rapidly dissipating in the central Texas-Oklahoma area as TIROS I passed over at 1624 CST. The cloud charts at 1600 CST, Fig. 10, show the agreement between the observations and the TIROS photograph. The most striking feature noted in the cloud evolution of the mesosystem is the large increase with time in the ratio of high cirriform clouds to low or precipitation-producing clouds. The active portions of the system are seen through radar and cloud observations.

The time variation of the mesosystems and the vertical and horizontal motions that account for such cloud formations will be examined in the next section.

5. TIME VARIATION OF THE MESOSYSTEM

A. PRESSURE

The life-history of an individual mesosystem can be summarized through

reference to an isochrone-excess-deficit pressure diagram. Such a figure was constructed, Fig. 11a, and shows the movement of the leading edge of the meso-system (solid line). The hourly pressure charts were then analysed in order to determine the pressure fluctuations produced by the disturbance. It has been noted, Fujita (1955), that characteristic pressure perturbations (excess and deficit) are produced by a squall line. Briefly summarized, these perturbations on the large-scale pressure field consist of a small high in the early stages of the system becoming larger and more intense until the system reaches maturity, then dissipating as activity decreases. Following the formation and intensification of the high pressure cell, a low pressure forms just to the rear of the high and expands and intensifies with time reaching its maximum development a few hours after the maximum development of the high. The hourly tracks of maximum excess and deficit pressure are also shown on the figure and illustrate these features. The maximum excess pressure produced by this system was about four millibars, the maximum deficit pressure was about three millibars.

B. HUMIDITY

In a recent study, Brown (1962) determined that the "humidity dip", first described in The Thunderstorm, was a mesoscale phenomenon and should be examined with respect to the life cycle of a squall line. Although its cause is not yet known, two possible mechanisms were suggested in The Thunderstorm for the explanation of the coexistence of precipitation and humidities less than 100% within the thunderstorm. The first was that cold precipitation particles within the downdraft, due to a vapor pressure gradient directed from the air to the water, dessicated the air in the downdraft. The second depended on the inability of the water droplets to evaporate rapidly enough to maintain saturation in the downdraft. A third, suggested by Brown (1962), depended on the amount of entrainment or mixing with the environment along the leading edge of the downdraft in the squall line. As the downdraft increases in magnitude, the rate of mixing should increase and the available time for obtaining equilibrium between the saturated and non-saturated air should decrease. The time variation of the humidity dip zone was examined through the hourly charts. Its position along the

leading edge of the line and in the zone of precipitation was determined, Fig. 2b and 3b. In addition, isochrones of the humidity dip zone were constructed and deficit humidity determined and analysed utilizing the same methods which are applied to excess and deficit pressure determination. The resulting time variation of the intensity and areal coverage of the dip, Fig. 11b, shows an interesting similarity to the time variation of excess pressure. This similarity will be discussed in the next section.

C. COMPARISON OF EXCESS AND DEFICIT PRESSURE WITH DEFICIT HUMIDITY

The analyses of squall lines have resulted in the establishment of the characteristic time variation of the excess and deficit pressures as mentioned in the previous section. A diagram (see also, Fujita (1962)), which shows the relationship of the excess and deficit pressure with time,is shown in Fig. 12a. This diagram illustrated that the time change cycle can be described in three separate legs. The first, from 0200-0800 CST shows the increase of excess pressure and a lesser increase of the deficit. The maximum excess pressure occurs at 0800 CST. Following this, the second leg consists of a rapid decrease in the excess pressure and a continued increase in the deficit until its maximum value is reached between 1000 and 1100 CST. The third leg illustrates the dissipation of the system and consists of a rapidly decreasing excess and deficit pressure.

Comparison of the humidity deficit with the excess pressure, Fig. 12b, revealed a different and interesting relationship. Noting that the variation of excess pressure is usually connected with the severity of the system it can be seen that the deficit humidity varies in almost the same manner, that is, the maximum humidity deficit and maximum excess pressure occur at almost the same time. Here again the cycle can be discussed in terms of similar paths. In this case, however, two paths suffice to describe the cycle. The first leg, a pressure increase, coincides with an increase in deficit humidity. The second leg, or excess pressure decrease, is accompanied by the decrease in the humidity deficit. Thus, even though the cause of the humidity dip is not yet known, it can be seen that a direct relationship exists between the presence and intensity variations of the dip and the intensity stages of the squall line. This

relationship is in agreement with the proposed causes of the dip; thus, before the various implications of the dip on the squall line can be discussed, more extensive information on the moisture variations prior to, during, and following squall lines must be examined. An attempt to obtain some of this information is detailed in another paper within this report.

6. HORIZONTAL AND VERTICAL DISTRIBUTION OF ATMOSPHERIC VARIABLES

At 0600 CST, May 30, as the mesosystem was approaching its mature stage of development, it was located within an area formed by upper-air observation stations at Midland (MAF), Amarillo (AMA), Abilene (ABI) and Roswell (RSW). The observations made by these and other stations over a larger area allowed for a fairly complete upper-air study of the squall line and its environment. A vertical display of constant pressure charts, Fig. 13, reveals several interesting features in the horizontal wind, temperature and moisture fields.

Streamline and isotach analysis of the winds on the various pressure levels, surface to 300 mb, revealed the variation of the wind field with height within the squall line and its environment. The surface environment winds are divergent; yet the topography, sloping up to the west, ensures forced lifting. The surface winds within the mesosystem are strongly divergent in the vicinity of the mesohigh. The meso-low is characterized by convergent winds.

The winds at 850 mb indicate a shift in the environment flow to the south and southwest; the existence of the mesohigh, as evidenced by the northwesterly wind at Midland; and the appearance of a low in eastern New Mexico, as evidenced by northwesterly winds at Roswell and southeasterly winds at Amarillo. The 700 to 400 mb wind field shows the tilt of the low to the west over the previously rain-cooled surface and lower-level air, and the presence of a narrow zone of relatively high-speed southwesterly winds over the active portions of the squall line. The high-level wind field, 300 mb, reveals an area of minimum wind speed and diverging streamlines over the active portion of the mesosystem.

The thermal structure of the squall zone can be described, through comparison of the Midland and Abilene soundings, as colder than the environment to the 500 mb level and warmer than the environment to the 250 mb level. The horizontal moisture

field, seen by the soundings at MAF, ABI and FWH indicates that the squall zone was embedded in a low-level moisture maximum and zone of convective instability.

7. VERTICAL DISTRIBUTION OF CONVERGENCE

In order to determine information on the vertical motion field, it was necessary to determine the convergence-divergence fields on the various pressure levels. The primary method utilized was the kinematic method, based on the analyses of streamlines and isotachs. The method utilized was essentially the same as that presented by Fujita (1955). In addition, in those areas where data were sparse, or such that an analysis tended to be subjective, the Bellamy (1949) objective technique was utilized, as a check on the limits of the values.

As an illustration of the computation of convergence, Fig. 14a shows the streamlines and orthogonals to the streamlines at the 700 mb level for 0600 CST. Mean values of winds along the orthogonals were obtained from the isotach analysis. Since, by definition, the streamlines are parallel to the winds, no component of motion is possible across the streamlines. Thus, determination of the net inflow or outflow in an area formed by two streamlines and two orthogonals and the respective area itself, leads to the evaluation of convergence through the equation

$$\text{Conv}_n V = \frac{V_u L_u - V_o L_o}{\Delta S}$$

A nomograph for the graphical determination of convergence values for various areas was given by Fujita (1955). The same method was utilized in constructing the nomograph, Fig. 26b. The left hand figure, on a plastic overlay, gives a quick value of the reciprocal of the area in question. The values of L and V, when entered along appropriate sections of the right hand figure, give values of VL. The difference, when multiplied by the reciprocal of the area, then produces the value of the divergence. The values of divergence for the various areas are indicated in the figure.

The vertical distribution of convergence through the squall zone and its environment is shown in Fig. 15a. Low-level divergence and upper-level convergence characterize the environment zone. The pre-squall zone indicates strong low-level convergence, changing to upper-level divergence. The active or leading edge of the

squall zone shows high values of divergence in the low levels, decreasing rapidly with height, and changing to convergence in the middle levels, then reversing again to strong divergence at the higher levels. The trailing, or wake low, portion of the system indicates large values of low-level convergence, decreasing rapidly with height, then increasing slightly through the middle-level low and becoming divergent again at the high levels. The final vertical section of convergence illustrates the return to low-level divergence and upper-level convergence at the rear of the squall zone.

8. VERTICAL MOTION COMPUTATIONS

Consideration of the conservation of mass in x, y, p coordinates results in an equation

$$\frac{\partial \omega}{\partial p} = D_p$$

which relates the height variation of the p-velocity ($\omega \equiv dp/dt$) with the divergence on an isobaric surface. Determination of the vertical velocity can then be achieved by stepwise integration of the mass conservation equation, such that

$$\omega_1 = \omega_0 + \int_{p_1}^{p_0} D_p \, \delta p$$

Thus, by utilizing mean values of D between pressure levels

$$\omega_1 = \omega_0 + \overline{D}_p \delta p$$

Applying the kinematic boundary condition; i.e., $\mathbb{V} \cdot n = 0$ at the surface,

$$\omega_0 \equiv \left(\frac{dp}{dt}\right)_0 = \left(\frac{\partial p}{\partial t}\right)_0 \cong 0$$

at sea level. Examination of the local pressure tendency within the mesosystem should be made for its contribution to the vertical motion field. In addition, the sloping topography should be considered by determining that

$$w = \mathbb{V} \cdot \nabla h$$

where h is the height of the earth's surface above sea level, or by

$$\omega = \mathbb{V} \cdot \nabla p_s$$

where p_s is the station pressure. However, for the present calculation ω_0 is

considered to be zero.

The results of the computations are presented in Fig. 15b. The envrionmental vertical motion field features descending motion (maximum at 500 mb); the pre-squall zone is characterized by ascending motion (maximum between 700 and 500 mb); the active portion of the squall zone by descending motion (possibly some ascent in the vicinity of the 500 mb level); the wake low portion of the squall by ascending motion; and to the rear of the mesosystem descending motion is again noted.

It should be emphasized that the vertical motion and divergence patterns are subject to wide variability since the divergence values are dependent on the areas involved in the computation and are also derived as a difference of two large numbers. Thus, errors in wind observations and representativeness of winds are quite important. An additional source of variability, which is difficult to assess in a study of this scale, is the variation of release time of rawinsondes. The times of release, for example, for the 0600 CST observations are shown in Fig. 13 at the 850 mb level. It can be seen that approximately one and a half hours elapsed between the earliest and latest observations. Thus, the convergence and vertical motion fields must be interpreted accordingly and are here represented more as indicative regions and areas of motion which require more intensive observation and study. For example, the horizontal and vertical extent of the pre-squall line convergent zone and the time change of the high-level divergent zone are specific cases, which should be examined in as great detail as possible, utilizing special rawinsondes and aircraft. Other areas of interest are the middle-level low located over the squall zone and the role that it plays in the life history of the mesosystem.

9. MOISTURE DISTRIBUTION AND THERMODYNAMICS

In order to examine in more detail the moisture distribution and thermodynamics involved in this squall-line-environment system, vertical soundings in various positions with respect to the mesosystem were plotted and are shown in Fig. 16. The thermodynamic diagram is a skew T - ln p presentation developed by Professor Fujita, in order to give a vertical presentation of temperature and a large angle between temperature and potential temperature. The solid lines (FWH, OKC) in both diagrams

are environment soundings. The Abilene (ABI) sounding (dash-dot) is also an environment sounding but in closer proximity to the squall system. The dotted lines (MAF, AMA) are squall soundings, and the remaining sounding at Albuquerque (ABQ) is representative of the environment to the rear of the disturbance. Winds are also plotted as a space representation of direction and speed changes.

Examination of the soundings reveals a number of interesting features. The environment soundings indicate a low moist layer capped by a temperature inversion and great convective, or potential, instability at Fort Worth and Abilene and to a lesser degree in Oklahoma City. The increase in height of the moist layer in the direction of the squall line is clearly shown by the two soundings at FWH and ABI. This feature has also been placed in the cross-section of Fig. 15b and shows agreement with the vertical motion field. It also indicates what might be the time change of the moist layer, as the disturbance moves from west to east. A clue to the dissipation of the squall line in the Oklahoma City area may be the lack of potential instability as evidenced by the OKC sounding.

The soundings within the disturbance (dotted lines) illustrate a low-level cold-air dome, which is a characteristic of mesosystems, and a high-level positive area (when compared to environment soundings) indicative of free convection. The winds indicate, as on the previous charts, Fig. 13, the low-level cold dome in the Midland (MAF) area, and the anticyclonic curvature ahead of the disturbance and the cyclonic curvature to the rear of the disturbance.

10. SUMMARY

In summary, analyses have shown that a squall line, which formed free of frontal activity, intensified and propagated through an atmosphere which was convectively unstable for a period of almost 24 hours and a distance of approximately 600 miles. Its maximum width (approximately 400 miles) and breadth (active portion about 100 miles) classify it as a larger mesoscale disturbance; yet experience indicates that this size is not unusual.

In addition to the customary parameters usually studied in a mesoanalysis of this type, two additional features were included. They were the utilization of TIROS

satellite photographs of the cloud systems attending the dissipating stages of a squall line and the attempt to relate the variation of the humidity dip with the life-cycle of the squall line. Both features added detailed information which had not previously been available. Both features indicate the need for and the possible means of continuing the study of the evolution of cloud systems of organized convective systems and the variation of the moisture field through squall lines.

The chance location of a convective mesosystem within an upper-air network at observation time allowed for a more detailed horizontal wind field and vertical motion study than is usually the case. The need is, however, pointed out for a more dense upper-air network and more frequent soundings in periods of expected convective activity. Zones or atmospheric volumes which are of particular interest with respect to the squall line were also pointed out. Some means of obtaining them, e.g., instrumented towers, were offered. Thus, the results not only indicate what has been achieved but also outline certain problems needing more intensive study.

REFERENCES

Bellamy, J. C., 1949: Objective calculations of divergence, vertical velocity and vorticity. Bull. Amer. Meteor. Soc., 30, 45-49.

Brown, H. A., 1962a: On the role of the humidity dip in squall line mesosystems. Semi-annual report, USASRDL Contract No., DA 36-039 SC88932, Dept. of Geophysical Sciences, University of Chicago.

Brown, H. A., 1962b: On the low-level structure of a squall line. Final Report, USASRDL Contract No. DA 36-039 SC88932, Dept. of Geophysical Sciences, University of Chicago.

Byers, H. R. and R. R. Braham Jr, 1949: The thunderstorm. U. S. Govt. Printing Office, Washington, D. C.

Cunningham, R. M., 1960: Hailstorm structure viewed from 32,000'. Physics of Precipitation, Geo. Mon., 325-332.

Fujita, T., 1955: Results of detailed synoptic studies of squall lines. Tellus 4, 405-436.

Fujita, T. and H. A. Brown, 1958: A study of mesosystems and their radar echoes. Bull. AMS, 39, 538-554.

Fujita, T., 1961: Outline of a technique for precise rectification of satellite cloud photographs. Technical Rep. to Weather Bureau, Contract No. Cwb 10047, Dept. of Geophysical Sciences, University of Chicago.

Fujita, T., 1962: A review of researches on analytical mesometeorology. Research Paper No. 8, Mesometeorology Project, Dept. of Geophysical Sciences, University of Chicago.

Whitney, L. F. Jr., and S. Fritz, 1961: A tornado-producing cloud pattern seen from TIROS I. Bull. Amer. Meteor. Soc., 42, 603-614.

Catalogue of meteorological satellite data-TIROS I, Television Cloud Photographs. 1961: U. S. Dept. of Commerce, Weather Bureau, Washington, D. C.

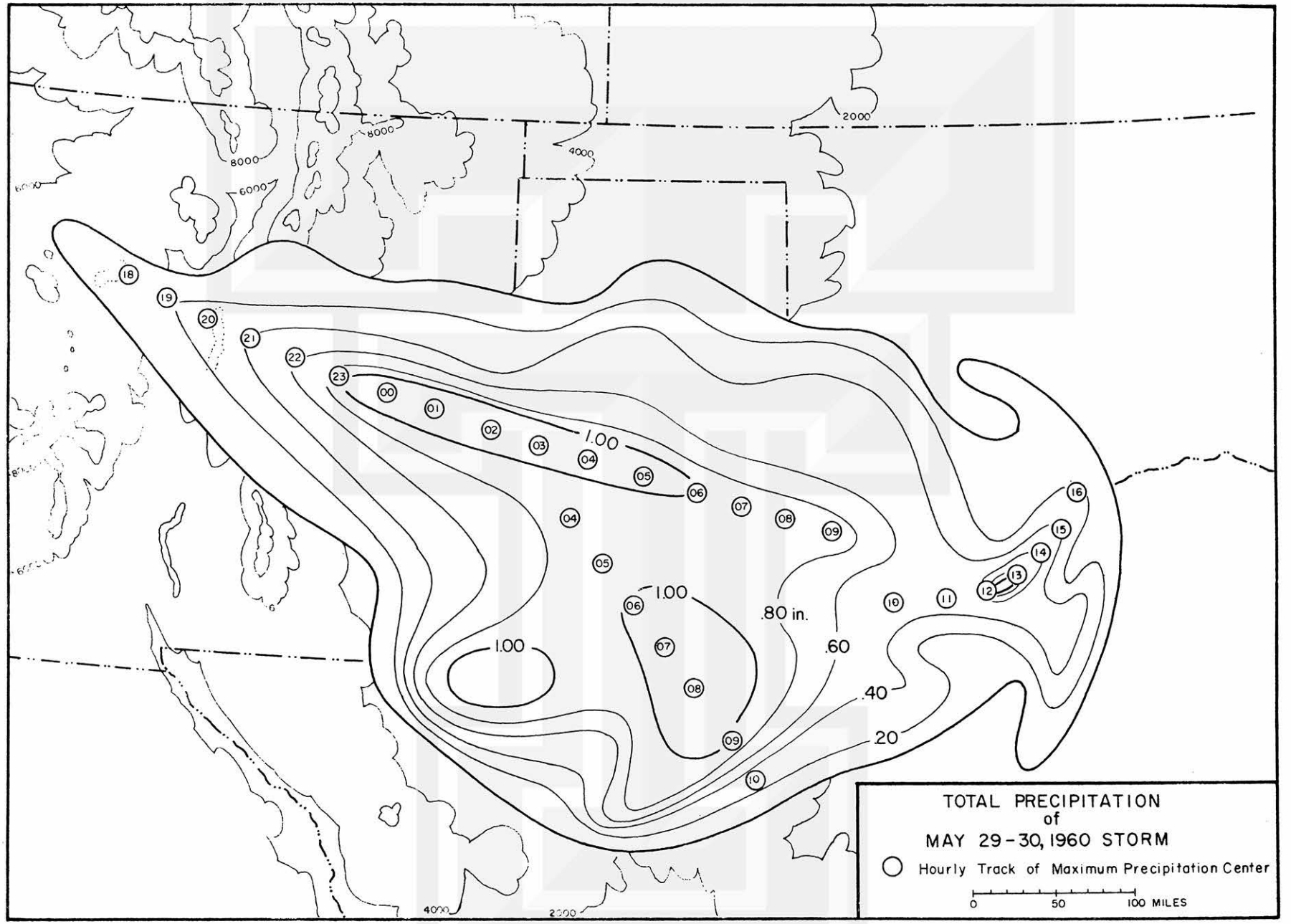

Fig. 1 Total accumulated precipitation of the May 29-30 storm.

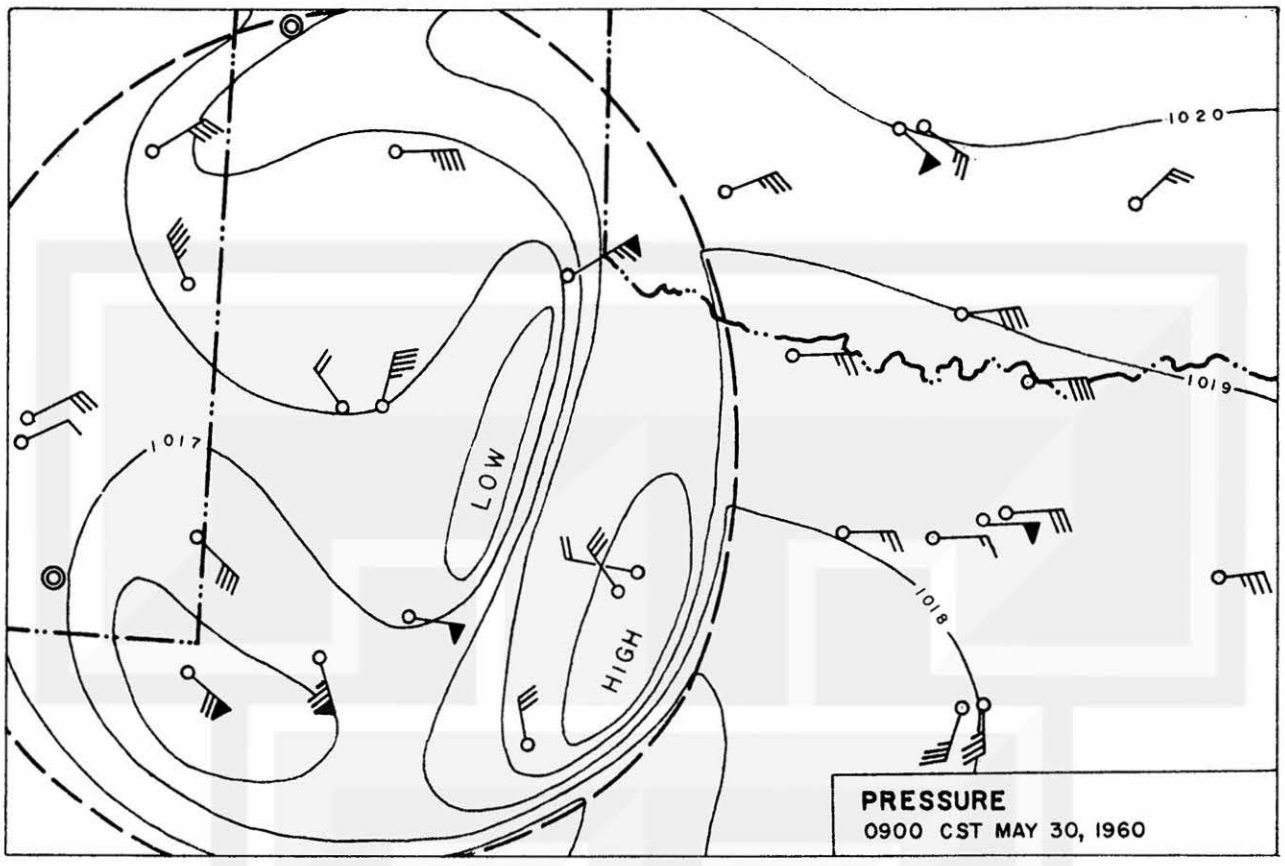

Fig. 2a Surface mesoanalysis of pressure. Boundary of mesosystem indicated by dashed line.

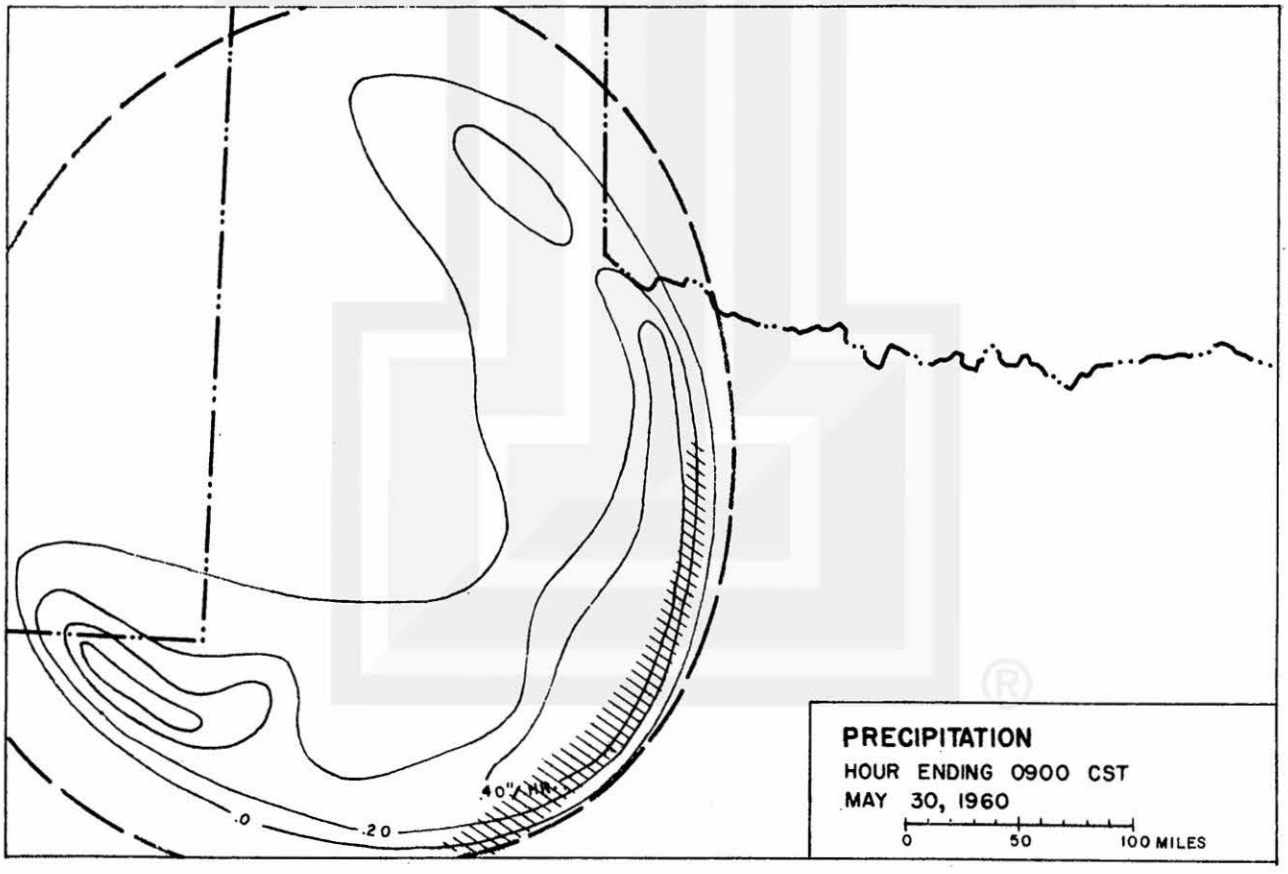

Fig. 2b Hourly amount of precipitation. Humidity dip zone at 0300 CST indicated by hatched zone.

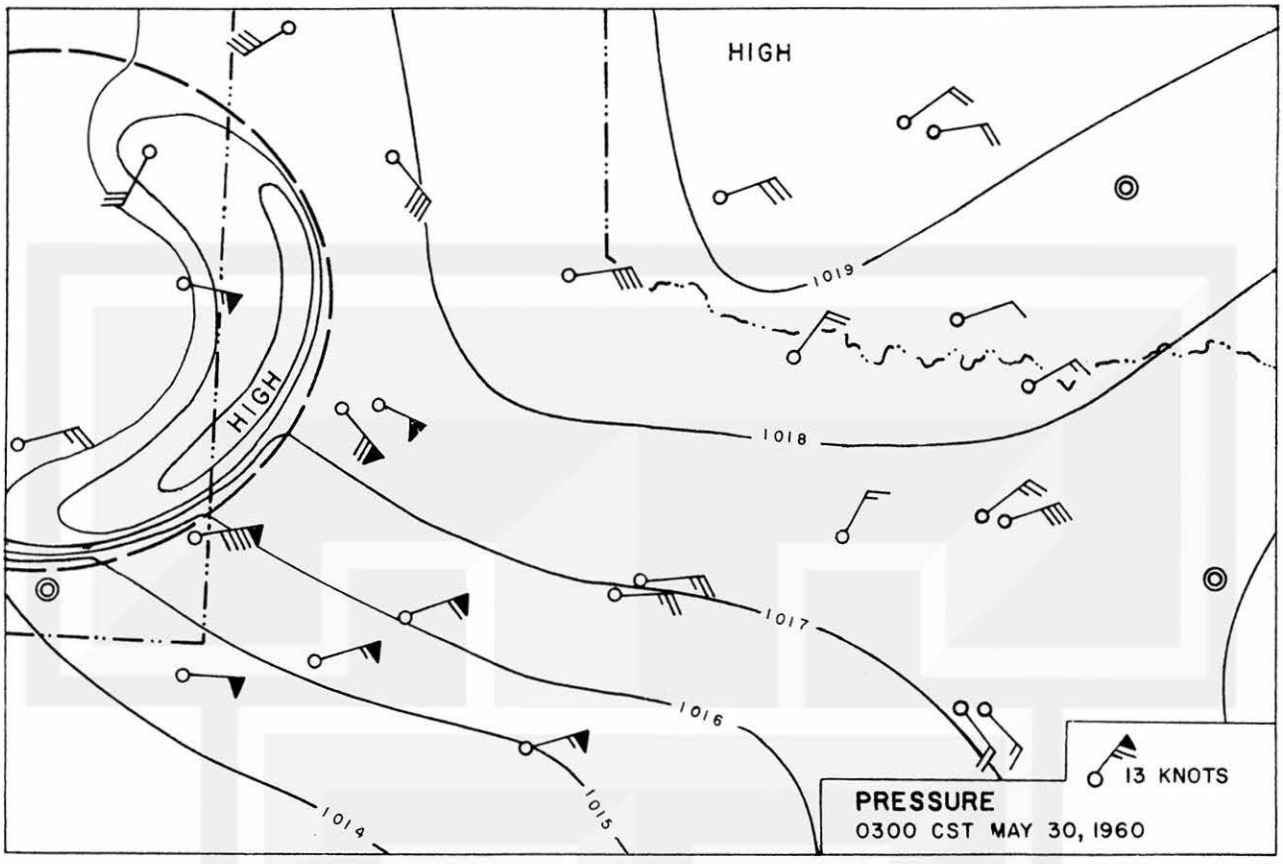

Fig. 3a Surface mesoanalysis of pressure. Boundary of mesosystem indicated by dashed line.

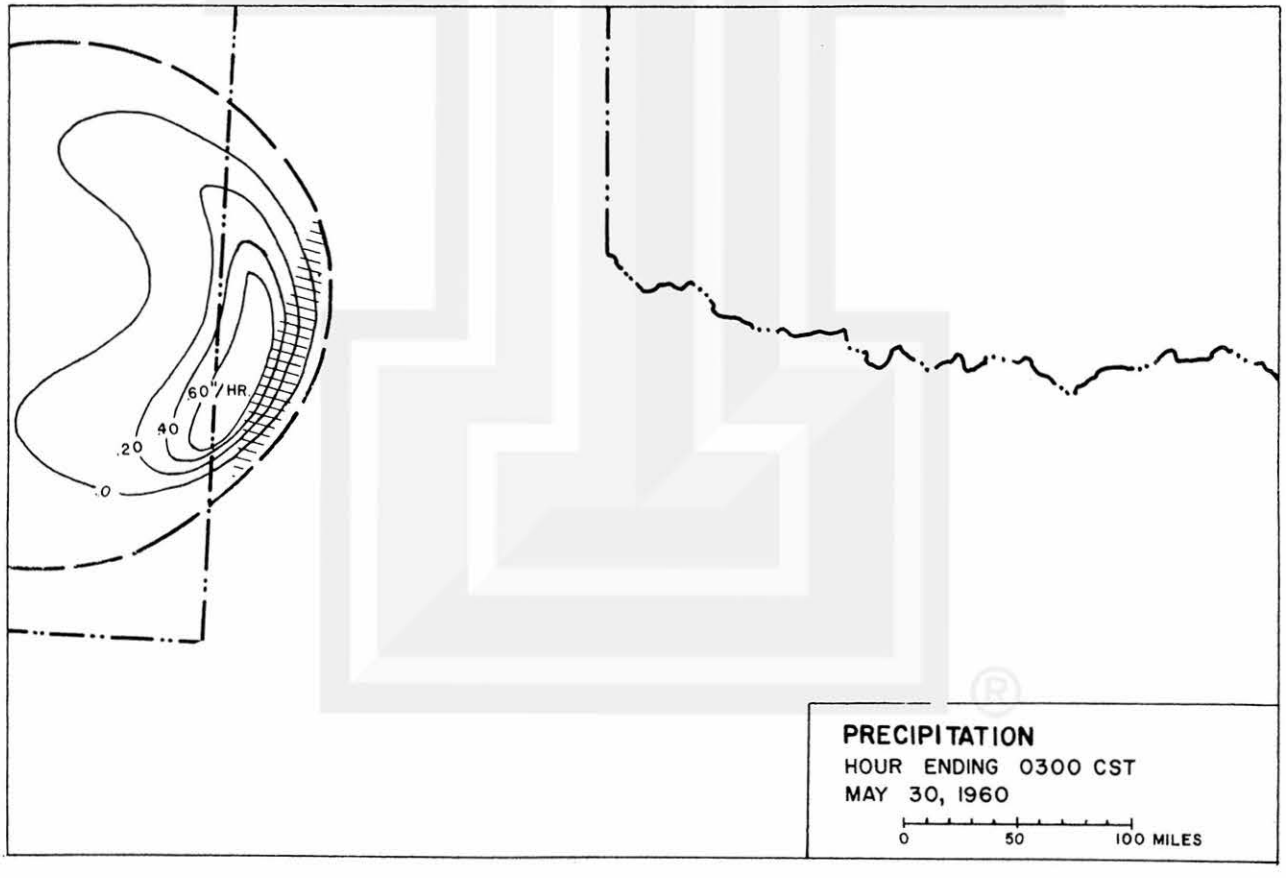

Fig. 3b Hourly amount of precipitation. Humidity dip zone at 0900 CST indicated by hatched zone.

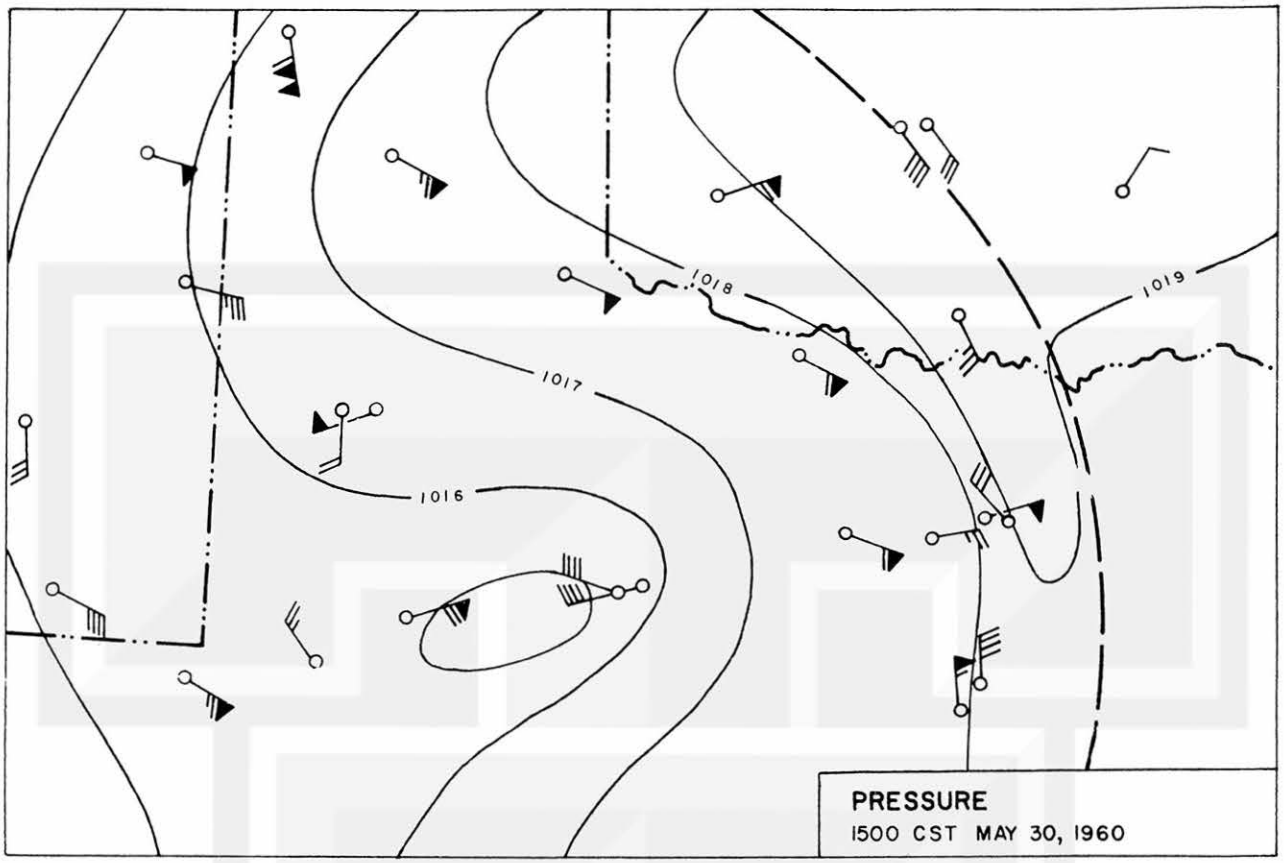

Fig. 4a Surface mesoanalysis of pressure. Boundary of mesosystem indicated by dashed line.

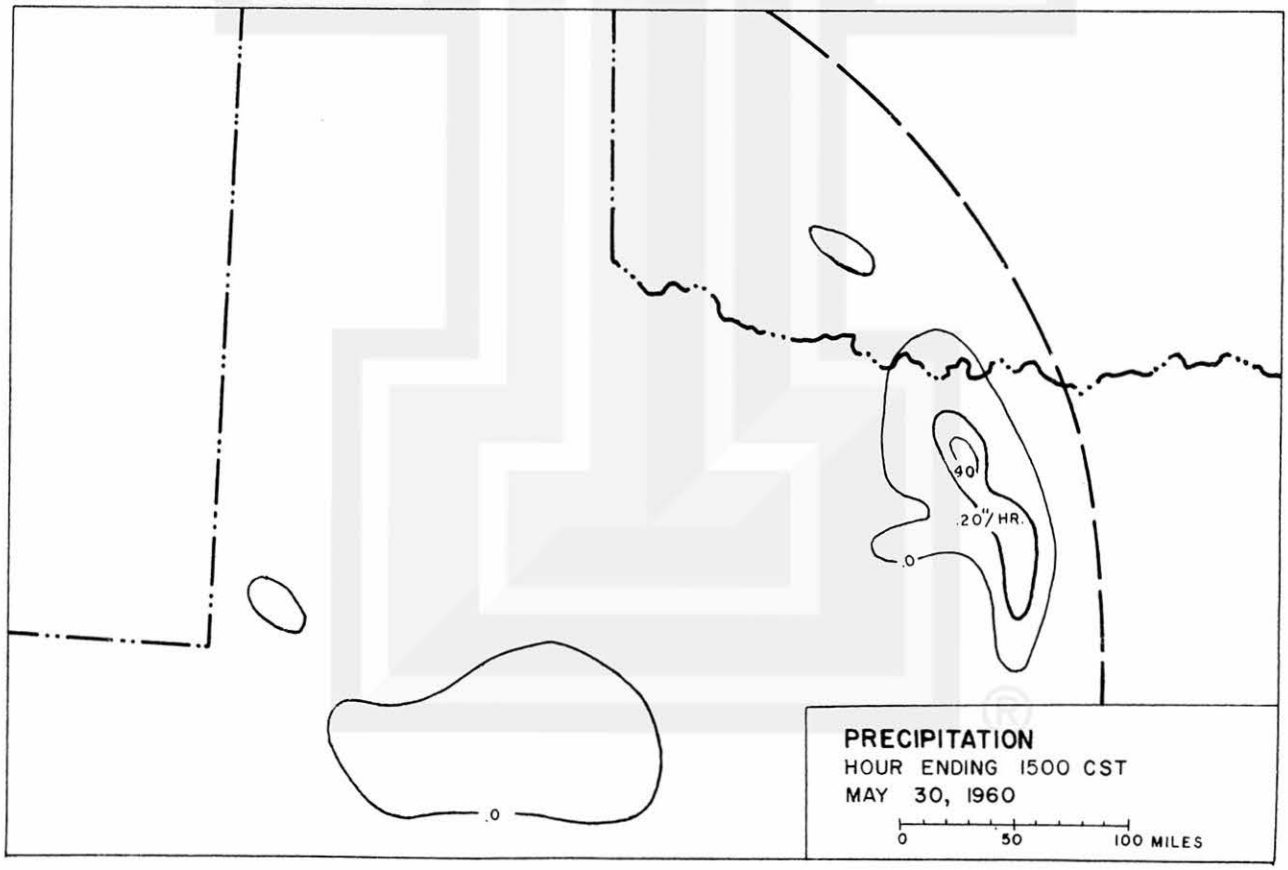

Fig. 4b Hourly amount of precipitation.

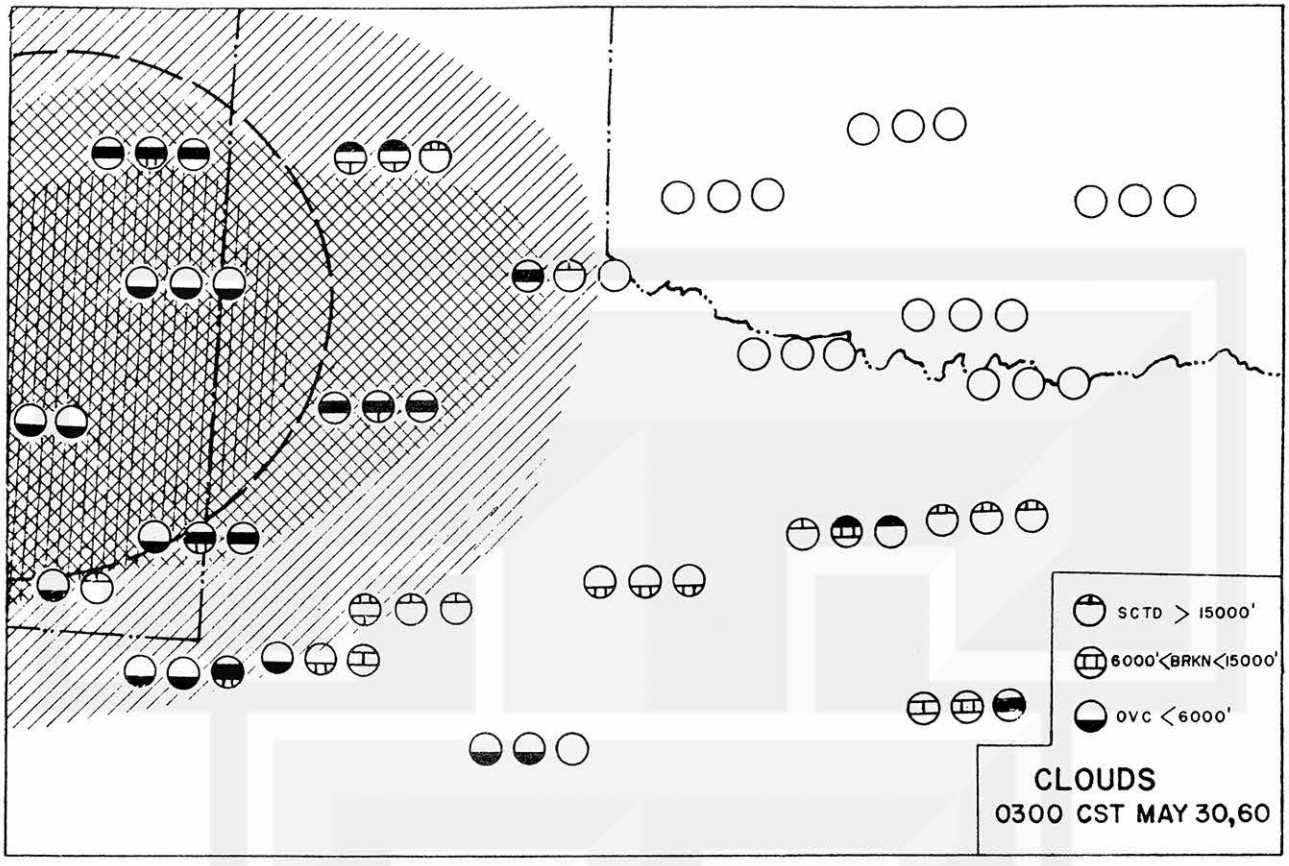

Fig. 5a Nephanalysis of mesosystem at 0300 CST. High clouds are indicated by single hatch zones, middle clouds by double hatch zones, and low clouds by triple hatch zones. Amount and height codes are shown in legend.

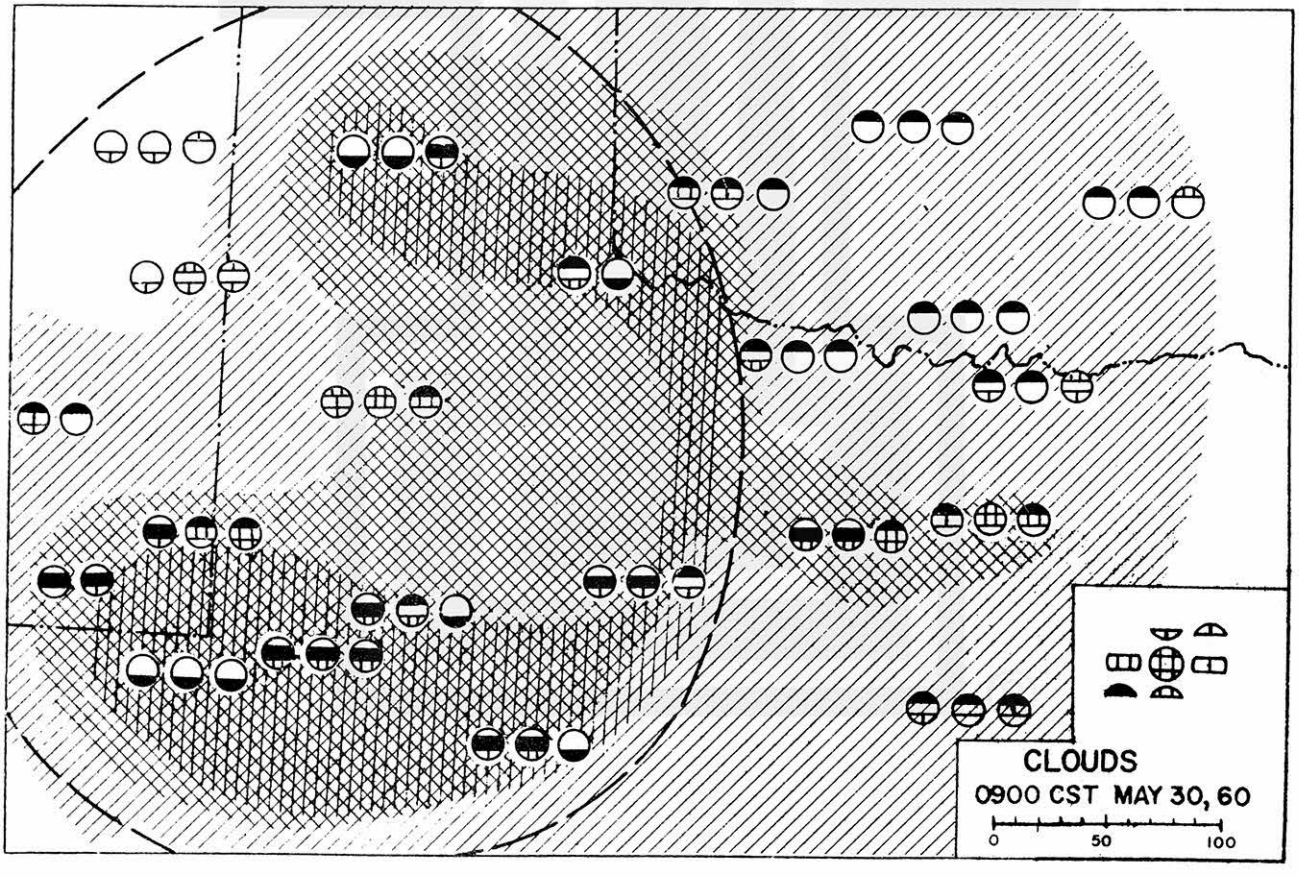

Fig. 5b Nephanalysis of mesosystem at 0900 CST. Symbols same as in Fig. 5a.

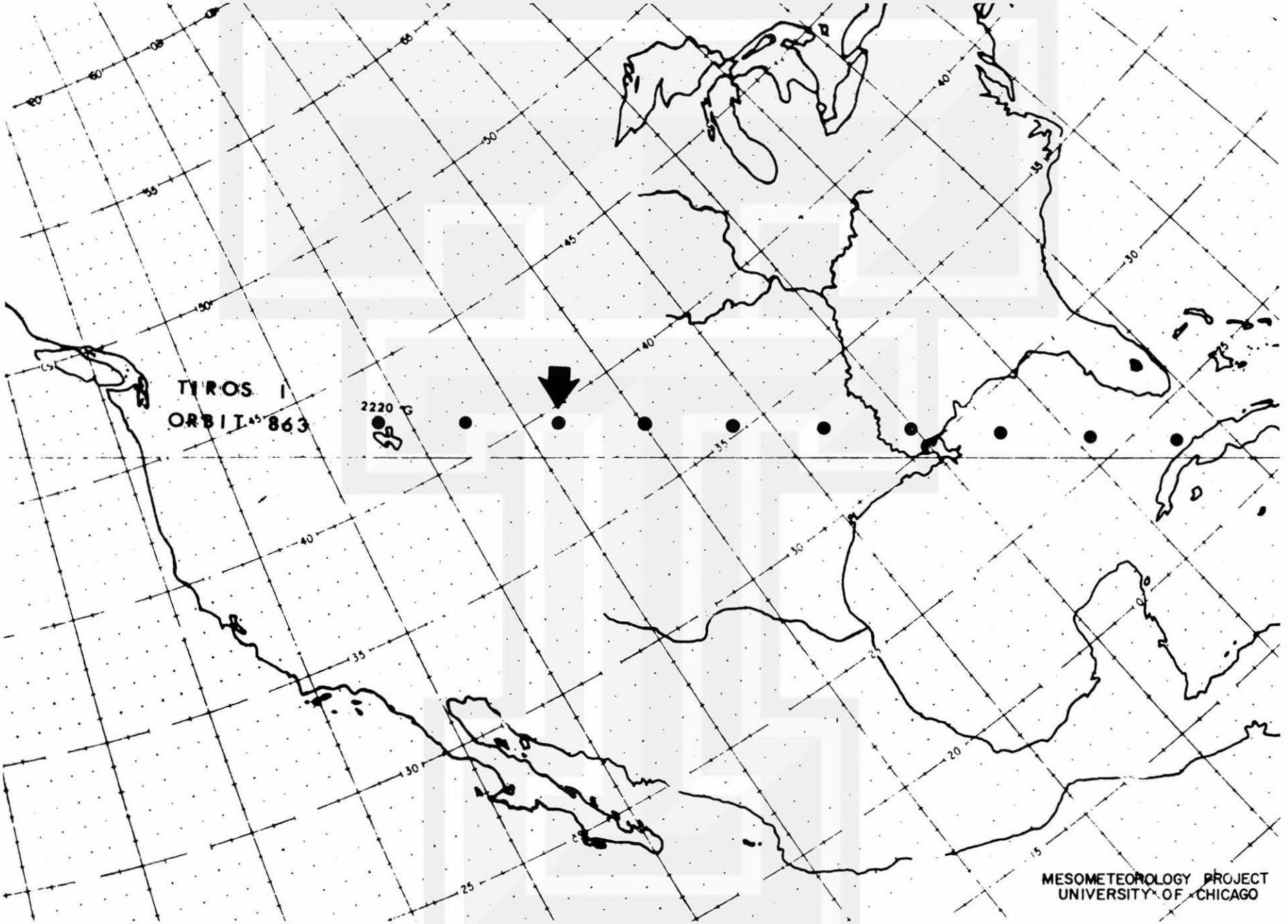

Fig. 6 Track positions of TIROS I during its 863rd orbit.

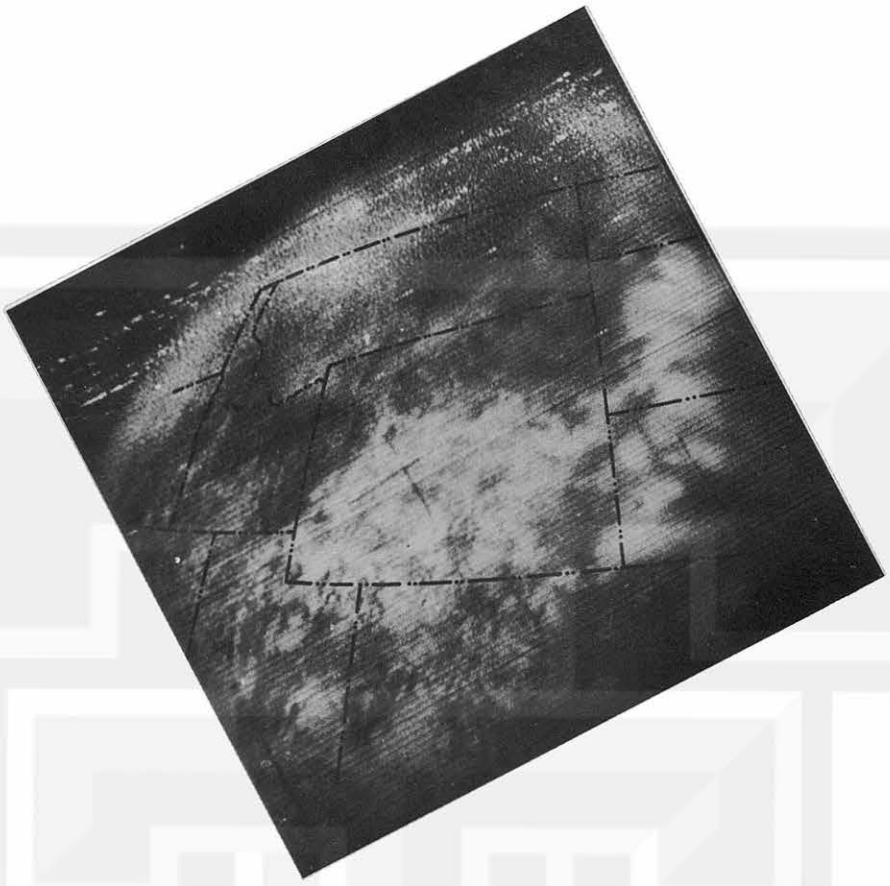

Fig. 7a Rectified satellite photograph taken at 16hr 22min 00sec CST showing clouds over Wyoming and surrounding states.

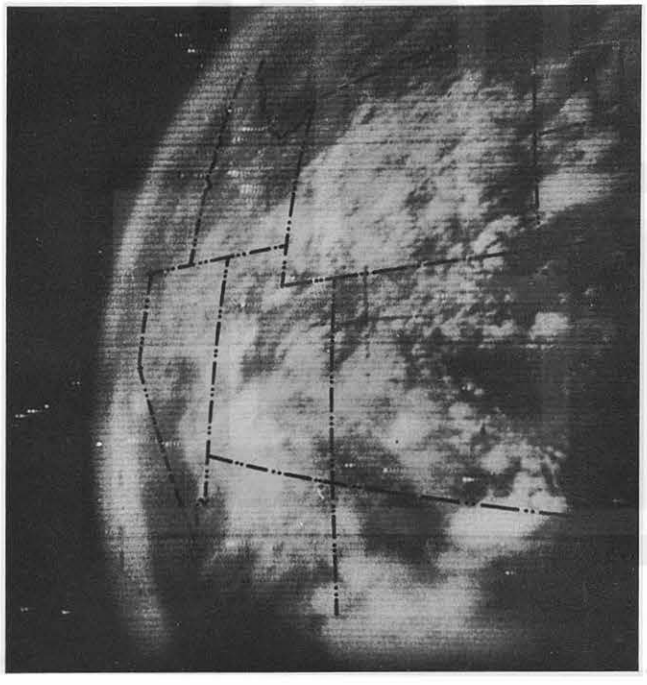

Fig. 7b Rectified satellite photograph taken at 16hr 22min 30sec CST showing clouds over Utah and surrounding states.

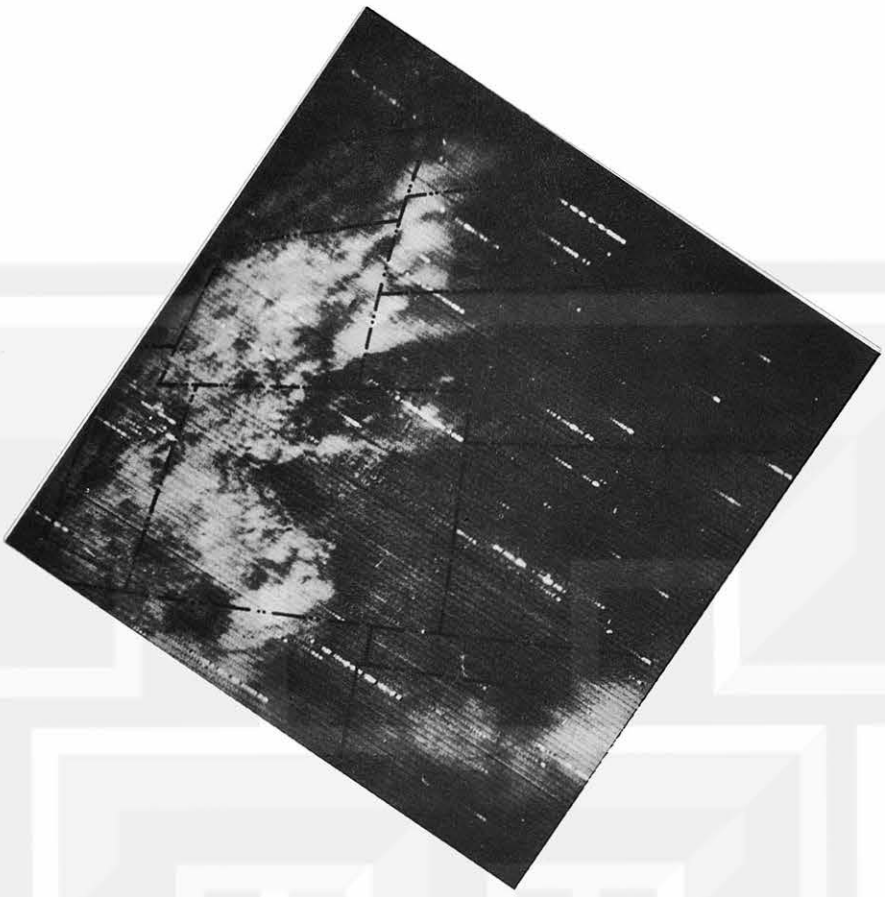

Fig. 8a Rectified satellite photograph taken at 16hr 23min 00sec CST showing clouds over Colorado and surrounding states.

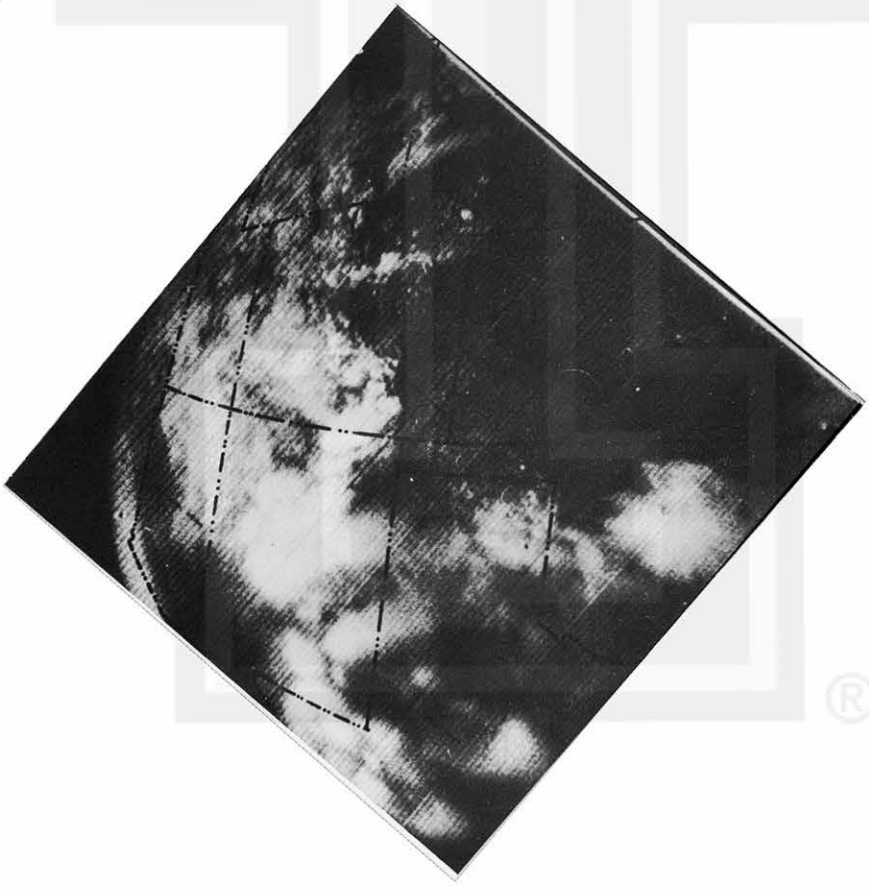

Fig. 8b Rectified satellite photograph taken at 16hr 23min 30sec CST over the Oklahoma-Texas Panhandles.

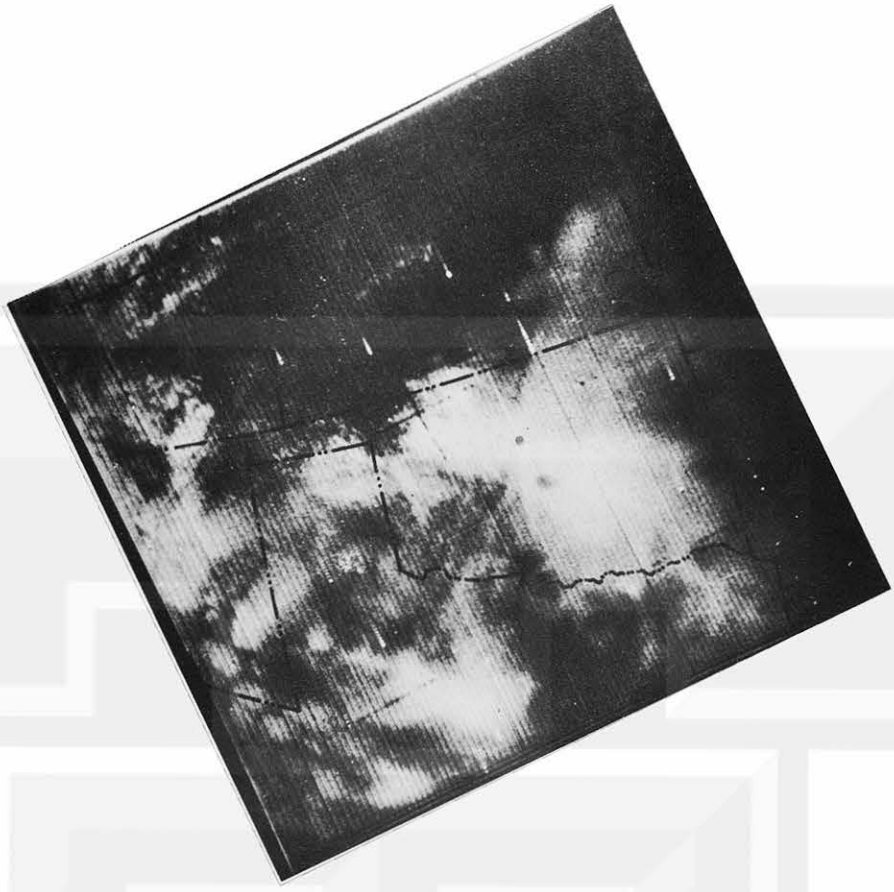

Fig. 9a Rectified satellite photograph taken at 16hr 24min 00sec CST showing clouds over Oklahoma and surrounding states.

Fig. 9b Rectified satellite photograph taken at 16hr 24min 30sec CST showing clouds over Oklahoma and surrounding states.

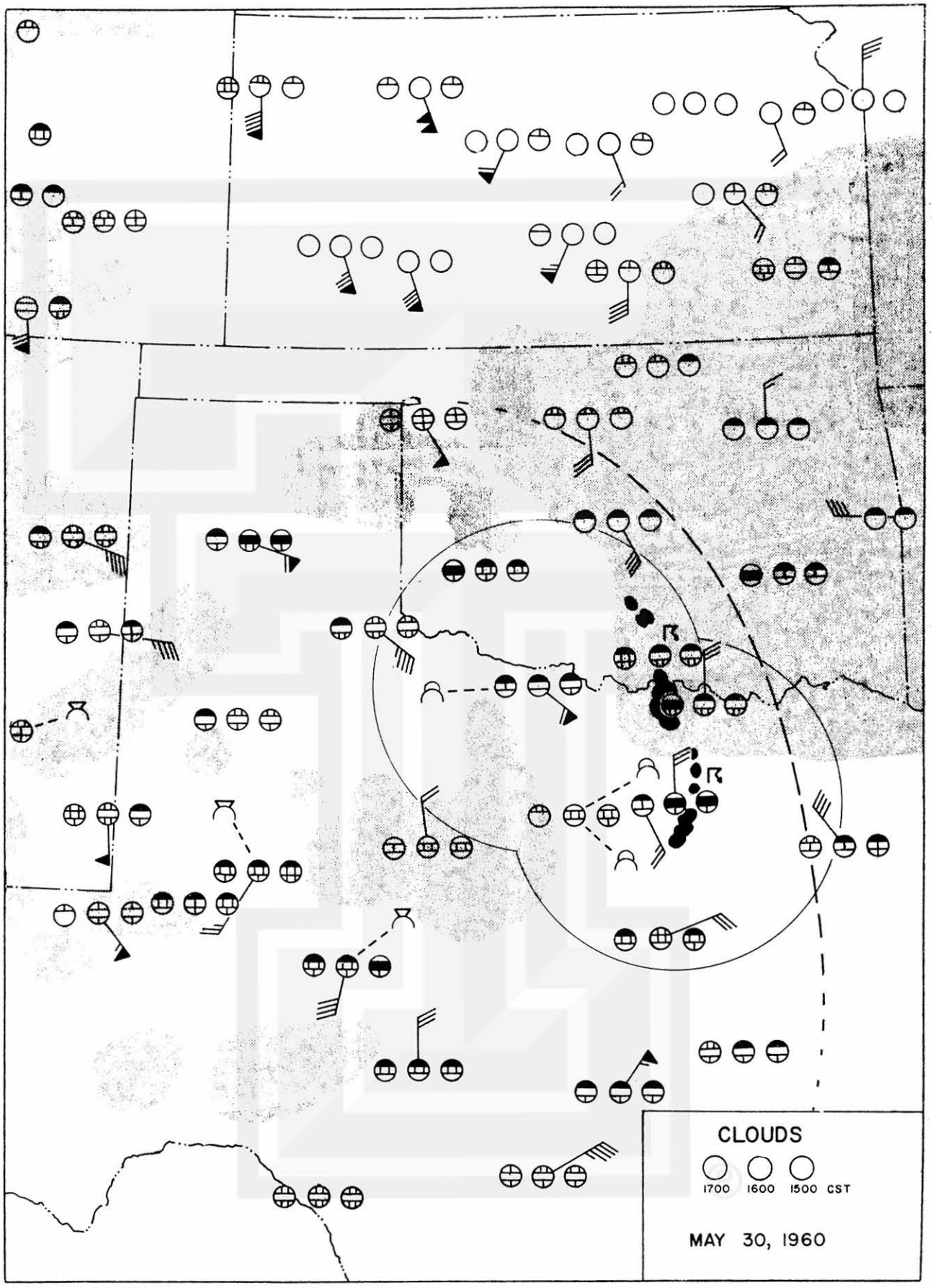

Fig. 10 Cloud and wind chart for 1600 CST. Shading represents cloud patterns as transformed from the satellite photographs. Cloud symbols are the same as in Fig. 5a. Wind barbs are equivalent to 2 mph, pennants to 10 mph. The boundary of the mesosystem is indicated by dash lines, the boundary of radar surveillance by circular zones, and the radar echoes at 1600 CST by the solid elliptical areas.

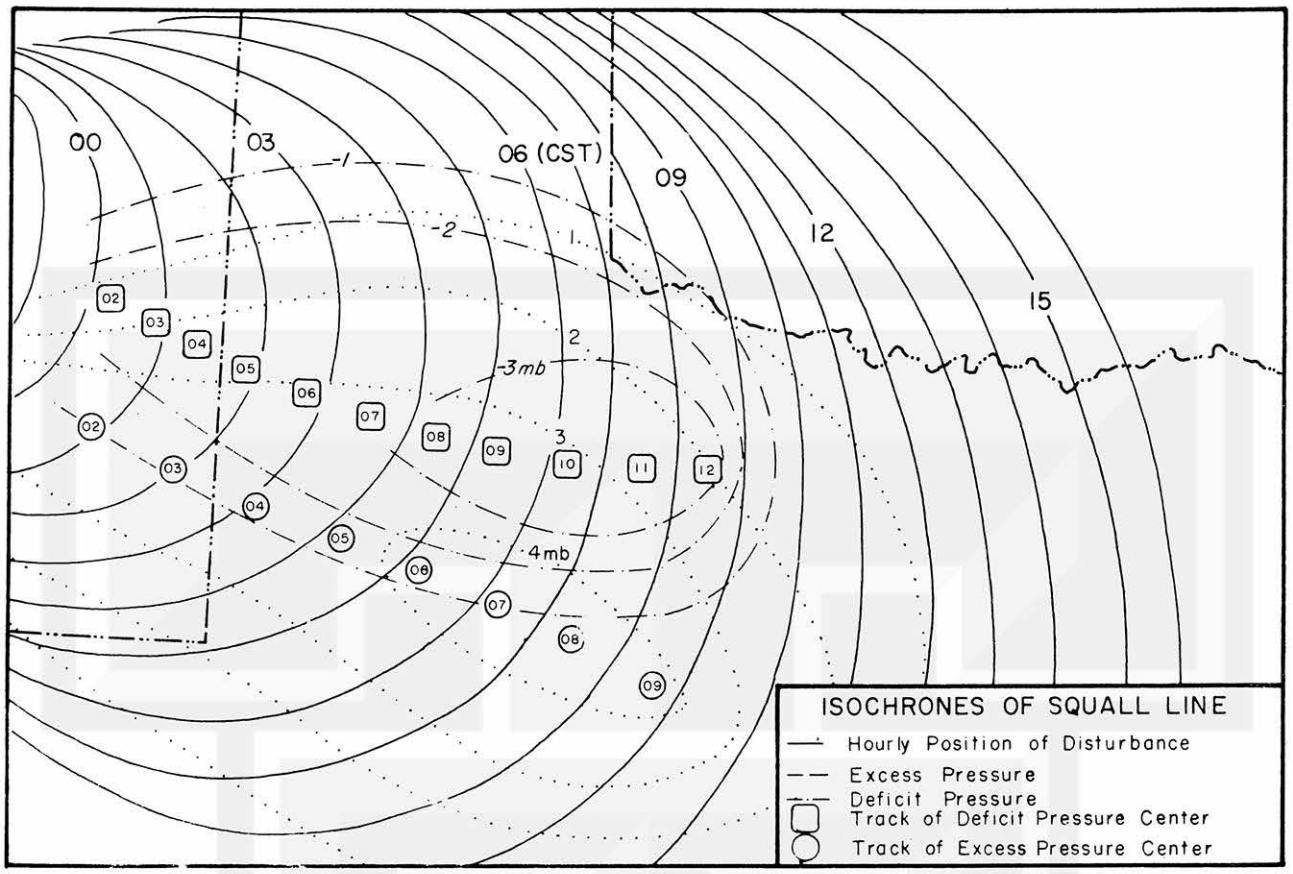

Fig. 11a Chart illustrating the history of the squall line mesosystem.

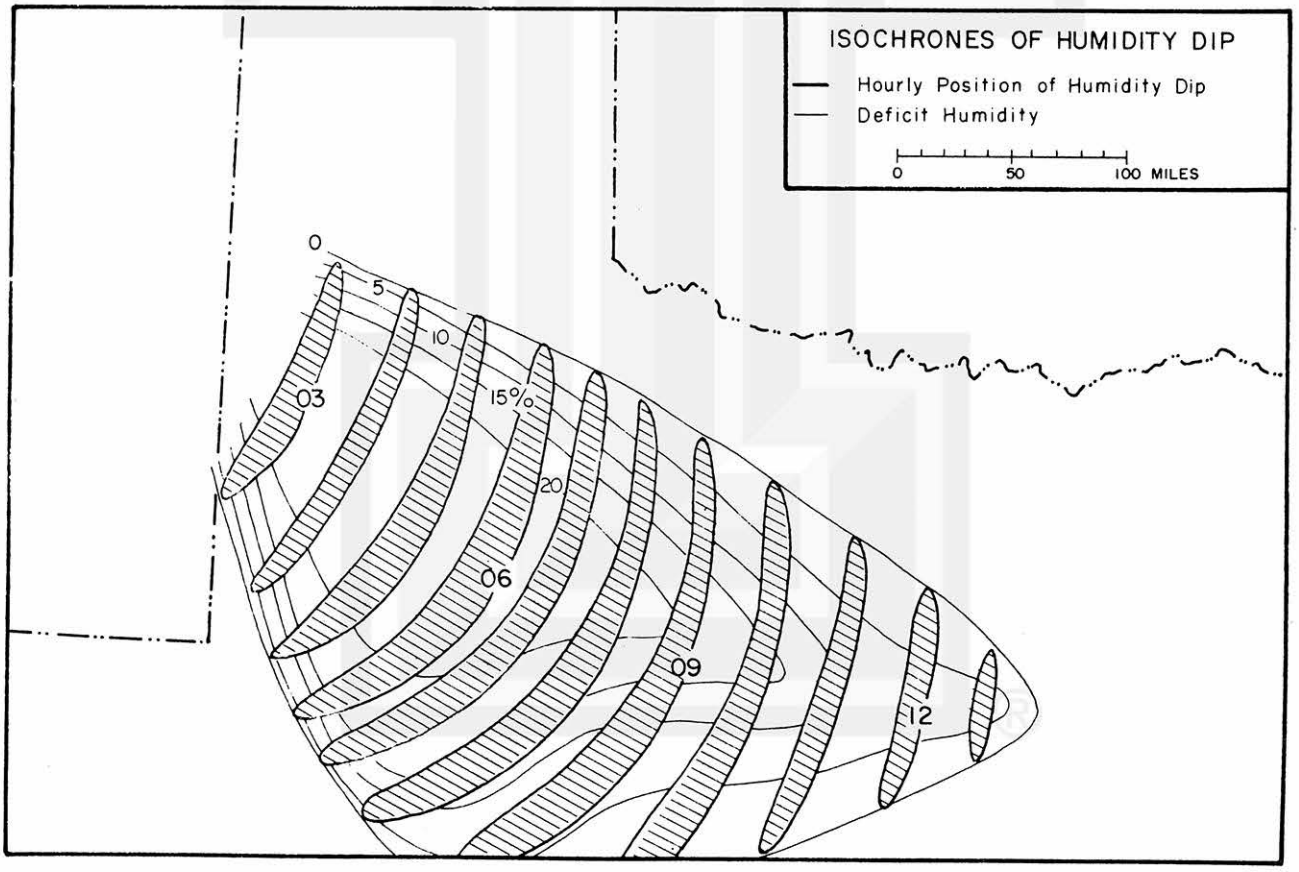

Fig. 11b Chart illustrating the history of the humidity dip.

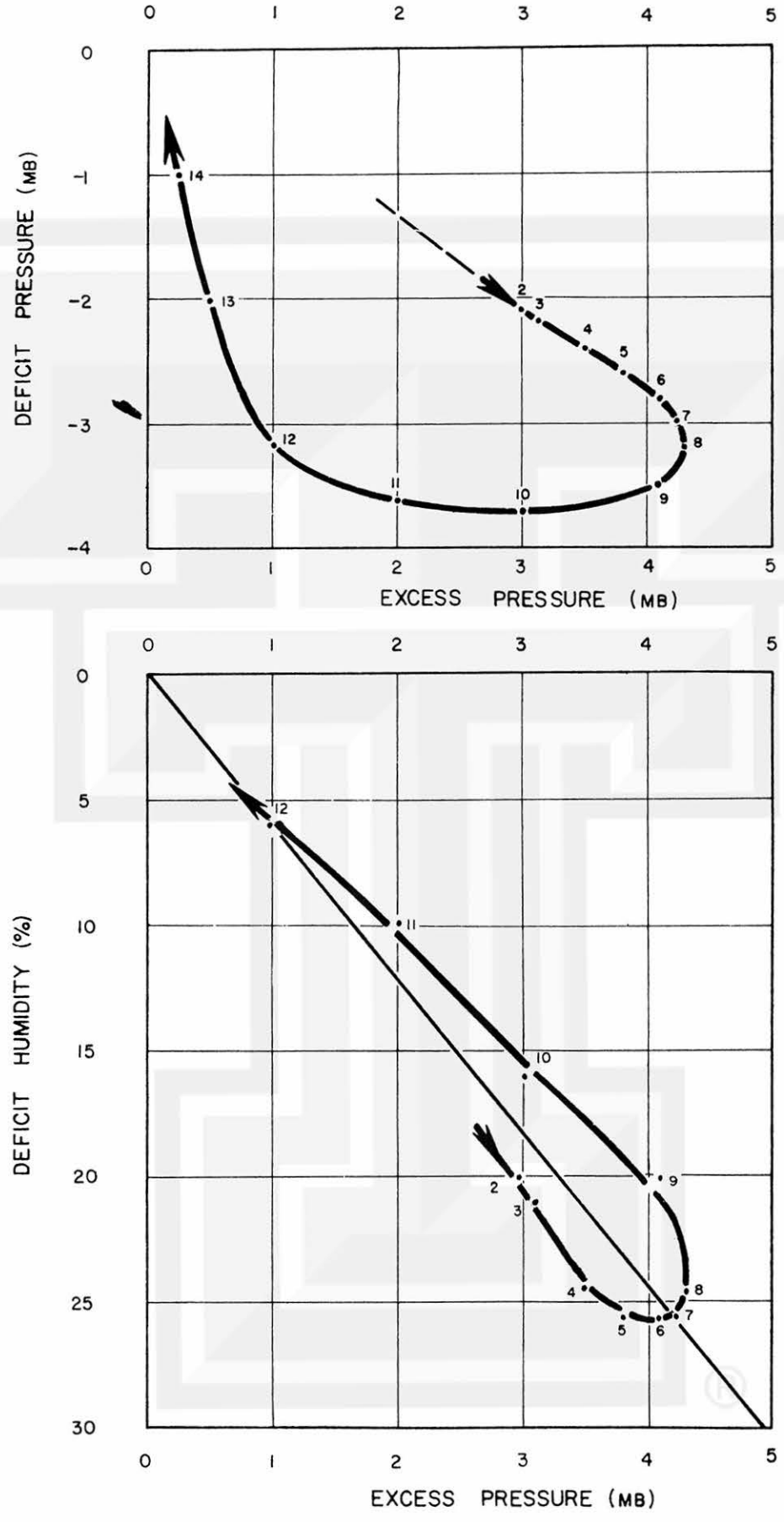

Fig. 12a Comparison between time variations of excess and deficit pressure (upper figure). Comparison between time variations of excess pressure and deficit humidity (lower figure).

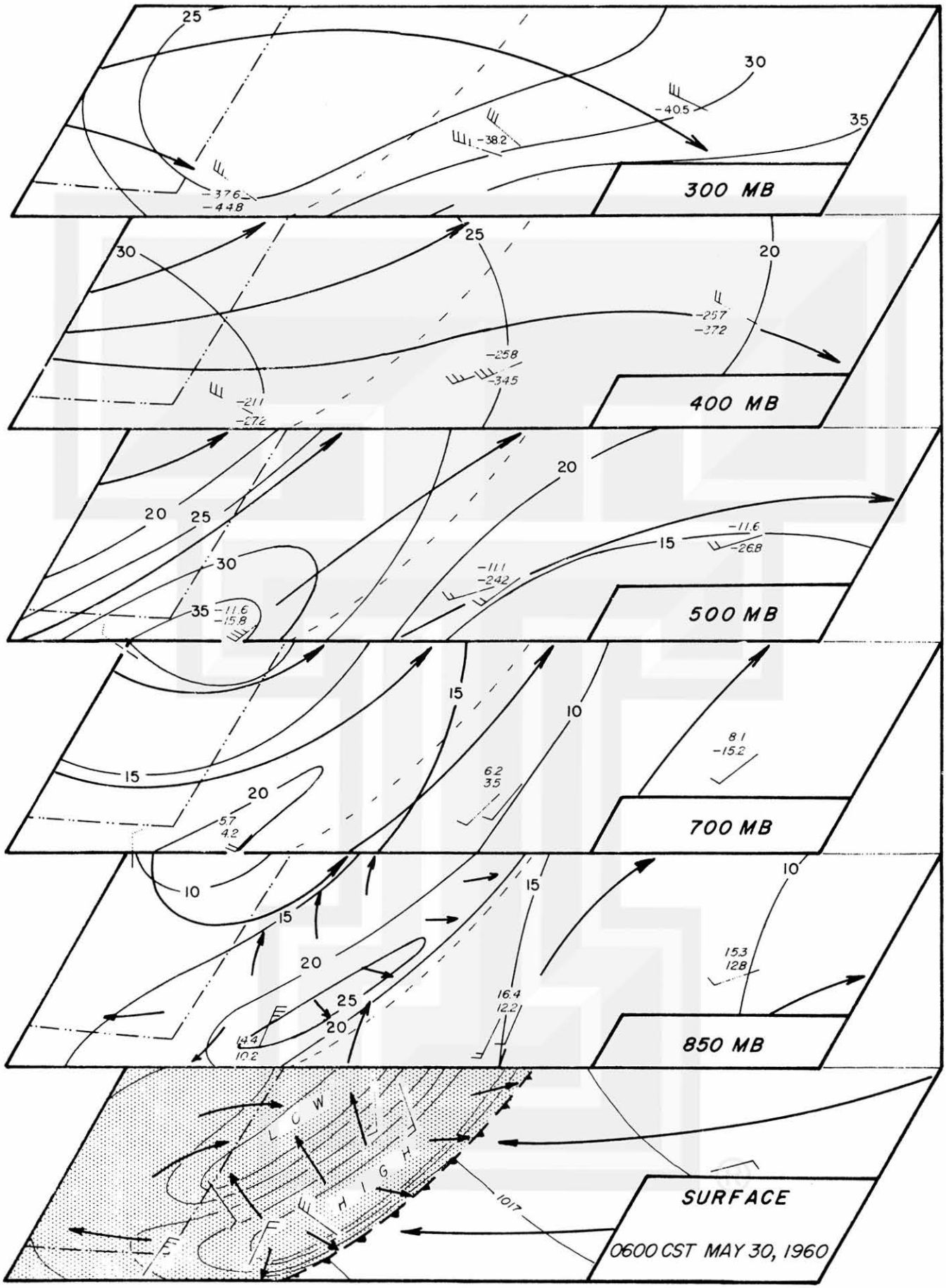

Fig. 13 Vertical distribution of winds and temperature on constant pressure surfaces in the vicinity of the squall line mesosystem (shaded area on surface map). The upper air observation stations are Midland, Abilene, and Fort Worth, Texas.

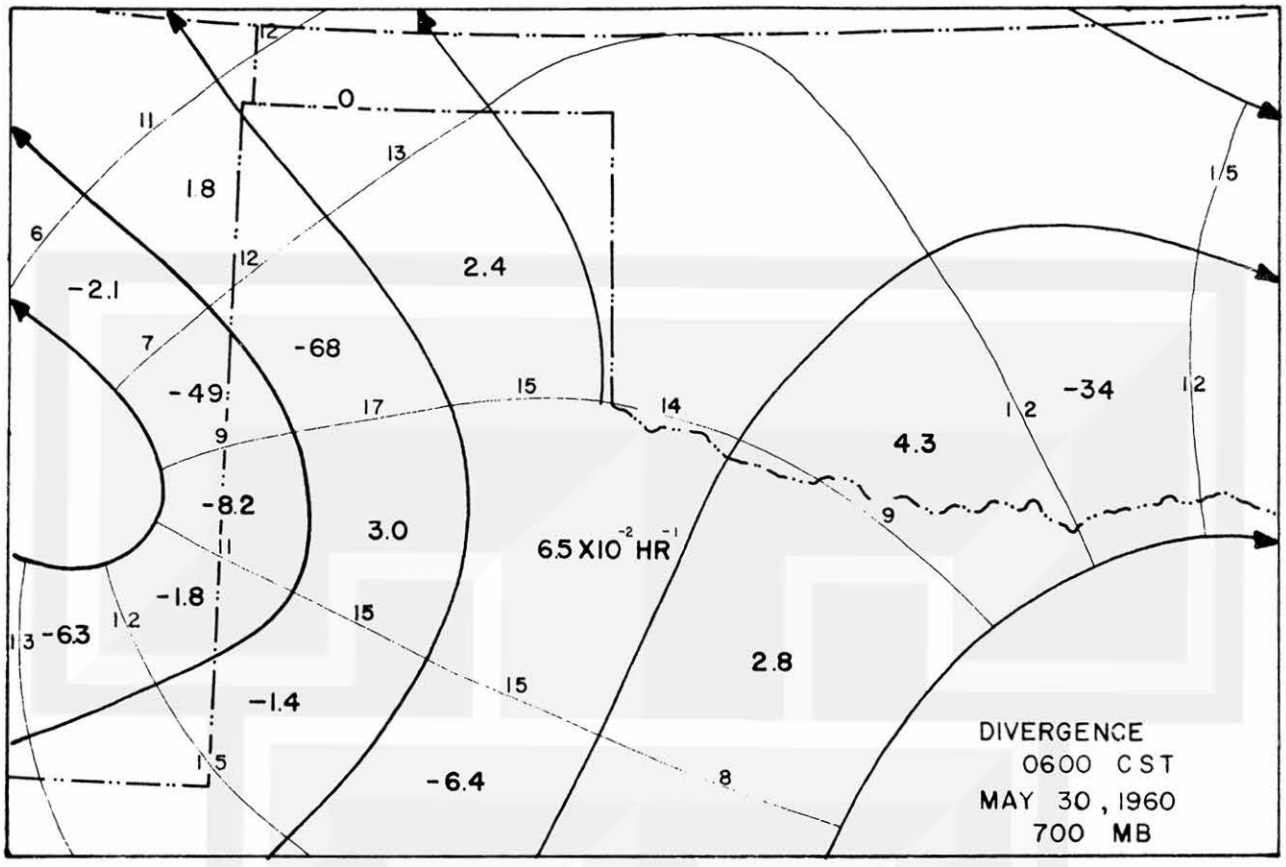

Fig. 14a Chart illustrating the streamline-ort'ıogonal method of computation of divergence. Small numbers represent the mean wind speed V along that section of tl e orthogonal L. Boldfaced numbers are the computed values of divergence.

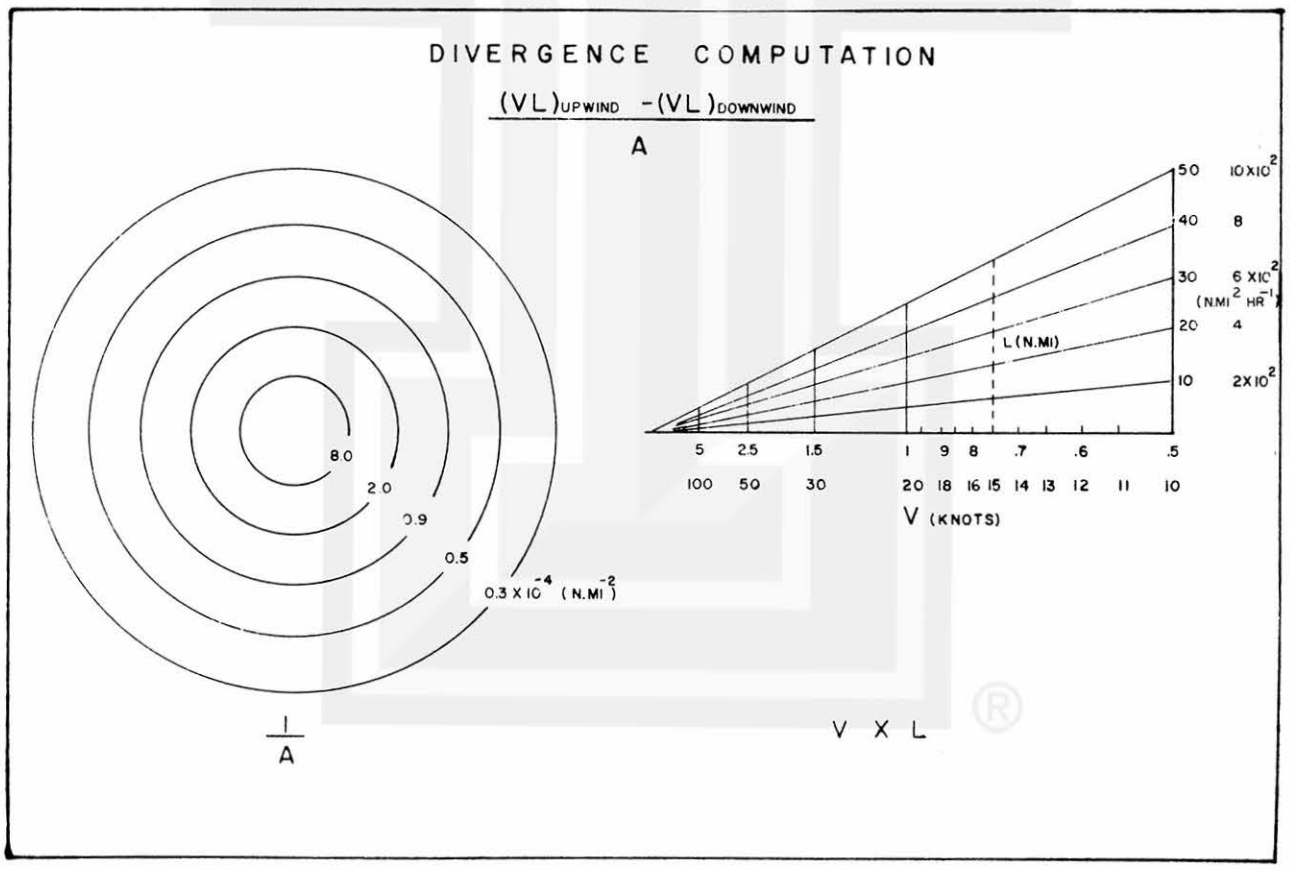

Fig. 14b Chart illustrating the nomograph utilized in computing the divergence from charts of the type illustrated in Fig. 14b. The mean speeds and lengths of the orthogonal between streamlines are multiplied in the right-hand graph; the reciprocal of the area under consideration is obtained from the left-hand overlay.

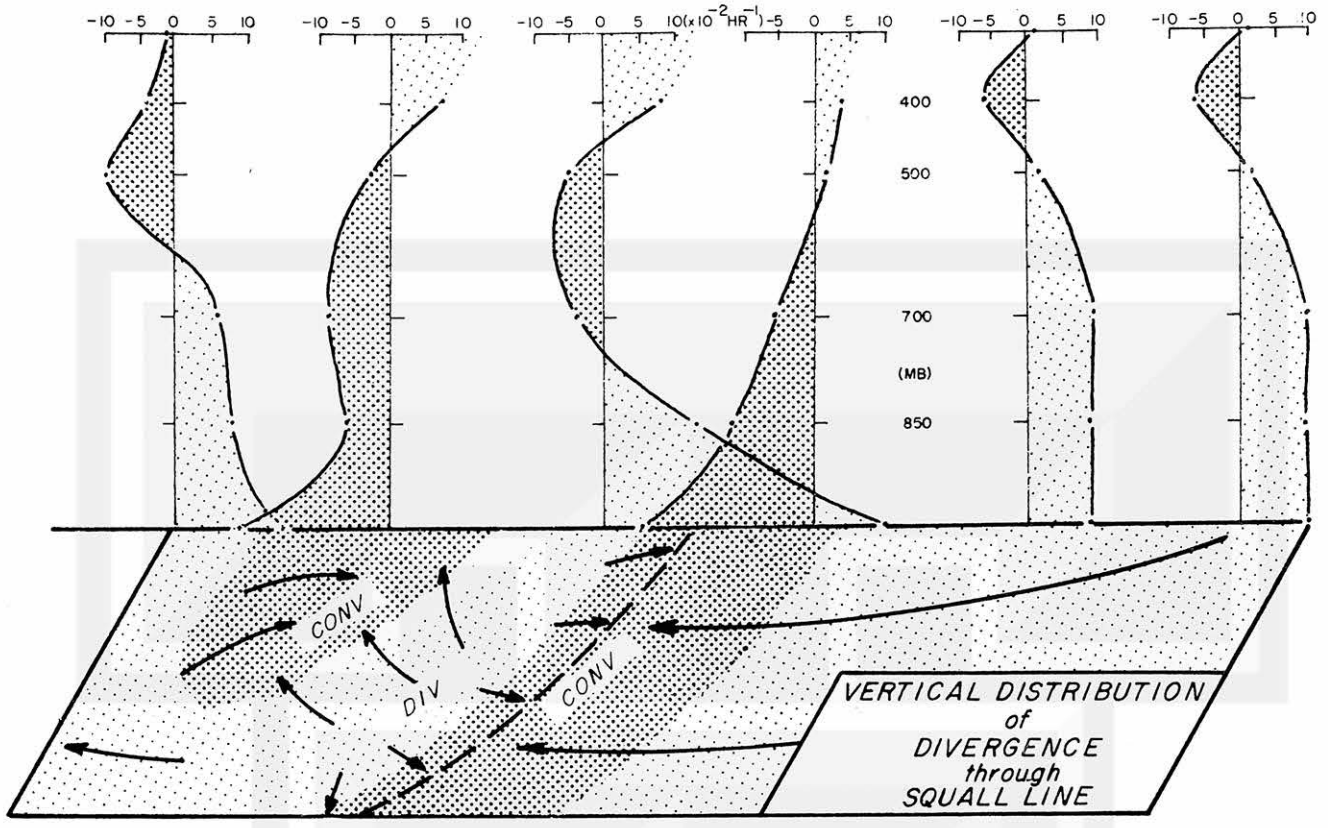

Fig. 15a Selected vertical profiles of divergence ahead of, within, and to the rear of the squall line mesosystem.

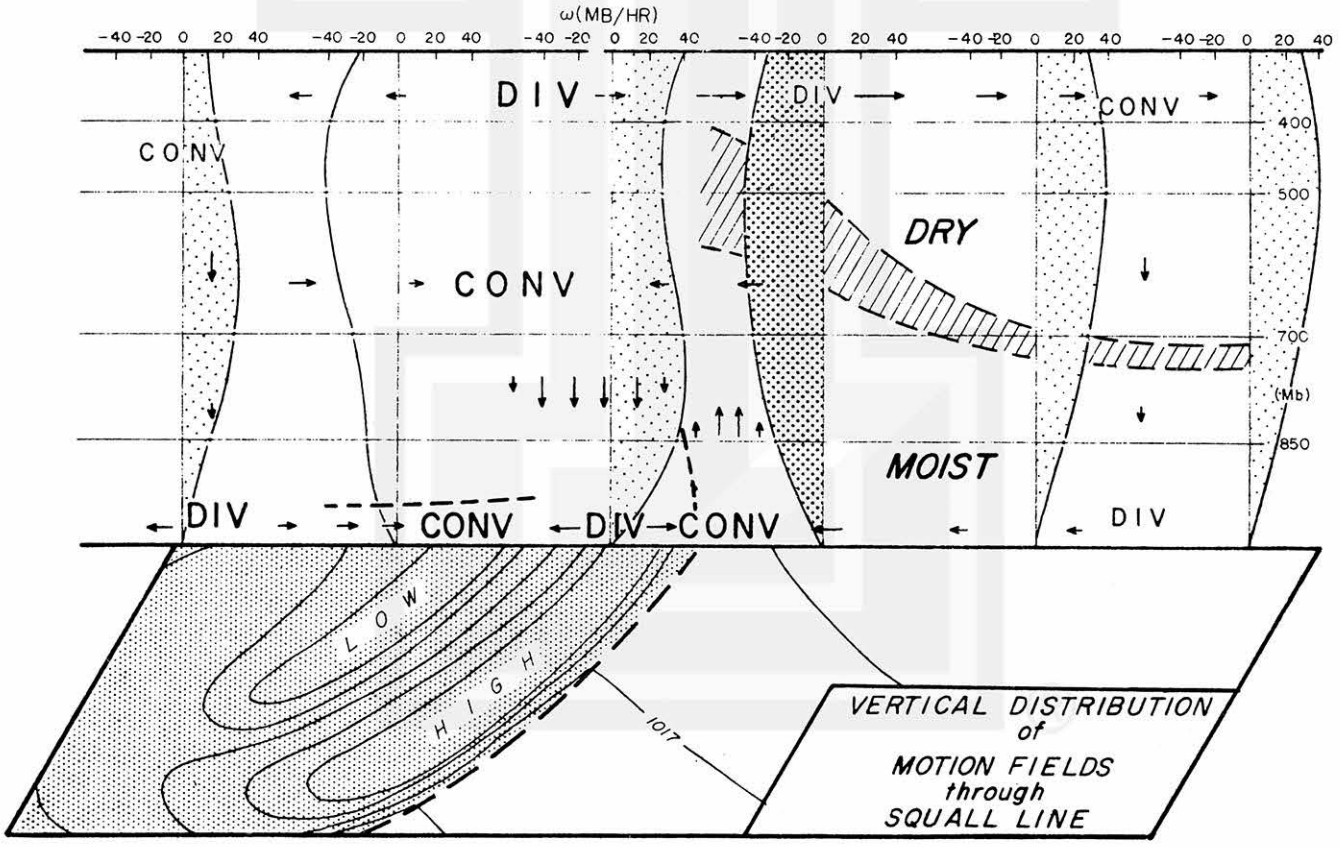

Fig. 15b Profiles of vertical motion obtained from the divergence profiles. The temperature inversion separating the moist from dry air is indicated by the hatched zone.

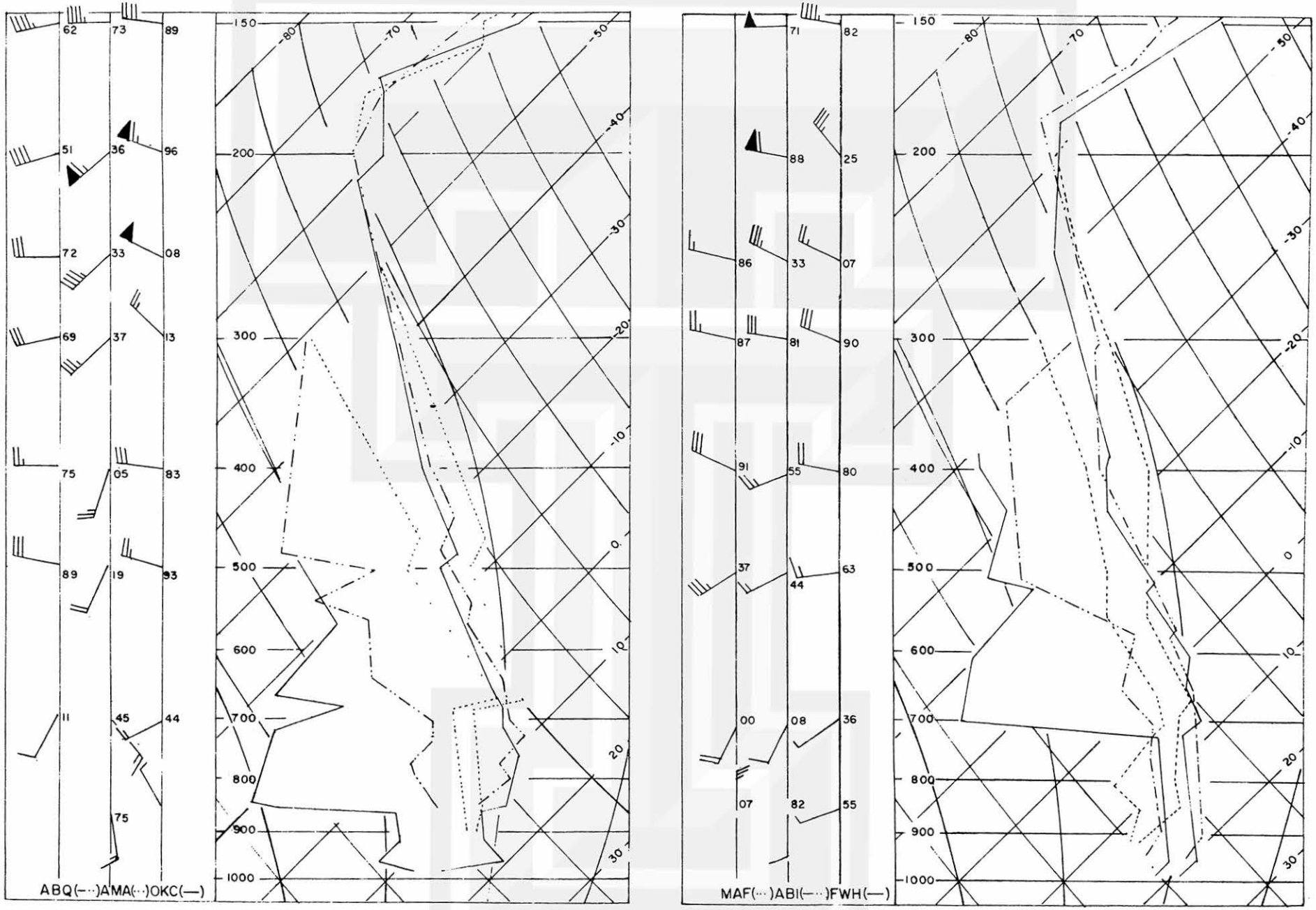

Fig. 16 Vertical distribution of temperature, dewpoint and wind ahead of the squall line (FWH and OKC), in close proximity to the squall line (ABI), within the squall zone (MAF and AMA) and to the rear of the squall zone (ABQ).

MESOMETEOROLOGY PROJECT ------- RESEARCH PAPERS

(Continued from front cover)

16. Preliminary Result of Analysis of the Cumulonimbus Cloud of April 21, 1961 - Tetsuya Fujita and James Arnold

17. A Technique for Precise Analysis of Satellite Photographs - Tetsuya Fujita

18. Evaluation of Limb Darkening From TIROS III Radiation Data - S. H. H. Larsen, Tetsuya Fujita, and W. L. Fletcher

19. Synoptic Interpretation of TIROS III Measurements of Infrared Radiation - Finn Pedersen and Tetsuya Fujita

20. TIROS III Measurements of Terrestrial Radiation and Reflected and Scattered Solar Radiation - S. H. H. Larsen, Tetsuya Fujita, and W. L. Fletcher

21. On the Low-Level Structure of a Squall Line - Henry Albert Brown

22. Thunderstorms and the Low-Level Jet - William D. Bonner